University of South Bohemia in České Budějovice

Faculty of Science

Department of Molecular Biology and Genetics

Assaying the effect of VEGFR2 receptor inhibition on preimplantation mouse embryo development.

Bachelor Thesis

Michael A. Holzer

Supervisor: doc. Alexander W. Bruce, Ph.D.

Co-supervisor: Lenka Gahurová, Ph.D.

České Budějovice, 2018

Holzer, M. A., 2018: Assaying the effect of VEGFR2 receptor inhibition on preimplantation mouse embryo development. Bsc. Thesis, in English, 51p., Faculty of Science, University of South Bohemia in České Budějovice, Czech Republic.

ANNOTATION

The aim of this thesis was to investigate the potential role of the Vascular endothelial growth factor receptor 2 (VEGFR2) in the cell fate decision in mouse preimplantation development.

DECLARATION

I hereby declare that I have worked on my bachelor's thesis independently and used only the sources listed in the bibliography. I hereby declare that, in accordance with Article 47b of Act No. 111/1998 in the valid wording, I agree with the publication of my bachelor thesis, in full to be kept in the Faculty of Science archive, in electronic form in publicly accessible part of the STAG database operated by the University of South Bohemia in České Budějovice accessible through its web pages. Further, I agree to the electronic publication of the comments of my supervisor and thesis opponents and the record of the proceedings and results of the thesis defense in accordance with aforementioned Act No. 111/1998. I also agree to the comparison of the text of my thesis with the Theses.cz thesis database operated by the National Registry of University Theses and a plagiarism detection system.

České Budějovice, 03.12.2018 …….

Michael A. Holzer

ACKNOWLEGDEMENTS

I would like to express my very great appreciation to supervisor Alexander W. Bruce, Ph.D. for giving me the opportunity to work in the field of Developmental Biology and Genomics. I appreciate his valuable and constructive suggestions during this work and analysis of the data. Beyond that he was willing to help me with any arising question throughout the theoretical as well as the practical part of the thesis and giving me a comfortable working space.

I would like to offer my special thanks to my co-supervisor Lenka Gahurová, Ph.D. for her professional guidance during my practical part. She always had an open door for questions and helped me in all times of research and writing. She was not only guiding me through my bachelor work but did enrich my stay in České Budějovice also on a personal level.

I also would like to thank Aleksandar I. Mihajlovic, Ph.D., Vasanth Thamodaran, Ph.D., and Giorgio Virnicchi, M.Sc., for their helpful support and for creating me a enjoyable working environment.

ABSTRACT

The zygote is the starting basis for the development of the embryo and its supportive tissues. For this, it is necessary that the descending cells differentiate in three distinct cell lineages during two cell fate decision events, by the time of uterine implantation (late blastocyst stage). The first cell fate decision induces the separation into inner cell mass cells (ICM) and extraembryonic trophectoderm cells (TE) which give rise to the placenta. During the second segregation process, the ICM lineage splits into the epiblast (EPI), a progenitor of the later embryo proper, and the primitive endoderm (PrE) which ultimately forms the yolk sac.

The question arises, which molecules and mechanisms organize this segregation processes. Various key elements are already studied, but more detailed research is needed to fully understand these crucial first steps in embryonic development. An approach to study these mechanisms is to compromise the function of individual factors and investigate their effects, this was also the basis for our experiments.

The element of our investigation was the Vascular endothelial growth factor receptor 2 (VEGFR2), a receptor known for its later function in vascular genesis. The role of the receptor during the preimplantation stage embryo cell fate decisions was examined by pharmacological inhibition with the compound Vandetanib; immuno-fluorescent staining for lineage marker protein expression was used to monitor effects on appropriate development at the blastocyst stage. In our experiments, we could not observe a role of VEGFR2 in regulating any of the particular lineage segregations, although a general developmental deceleration was detected. In higher concentrations, chemical blockade of VEGFR2 induced confirmed cellular apoptosis.

LIST OF ABBREVIATIONS

AFP	Alphafetoprotein
BSA	Bovine Serum albumin
DAPI	4,6-diamino-2-phenylindole dilactate
DMSO	Dimethylsulfoxide
EPI	Epiblast
FITC-Con A	Fluoresceinated Concanavalin A
hCG	Human chorionic gonadotropin
ICM	Inner cell mass
IF	Immuno-fluorescence
PBST	Phosphate-buffered saline Tween20
PrE	Primitive endoderm
PFA	Paraformaldehyde
PMSG	Pregnant Mare Serum Gonadotropin
TE	Trophectoderm
TF	Transcription factor
ZGA	Zygotic genome activation

TABLE OF CONTENT

1. INTRODUCTION

A zygote is formed after the fertilisation of the oocyte by the sperm – a single cell, which contains all the information necessary to constitute a life form. During development, the organism has to undergo various differentiation processes, with the first two cell fate decisions in mammalian embryogenesis taking place during the preimplantation stage. At the beginning of the preimplantation period, the embryo has a high resistance against experimental perturbations. This is caused by the high plasticity and self-organization of the embryo at this stage. An example of such high resistance/ plasticity is given by the fact that the removal of one cell at the 2-cell stage can be compensated by the remaining cell to specify the full developmental program. Moreover, experiments showed that the blastomeres of two distinct mouse preimplantation stage embryos can be seemingly reorganised as a single aggregate embryo, and successfully form a single chimeric adult mouse. An important part in this context is the early onset of the zygotic genome activation (ZGA). ZGA describes the point when developmental control of embryogenesis passes over from the maternal to the embryonic side (reviewed in C. Chazaud & Yamanaka, 2016; reviewed in Mihajlović & Bruce, 2017; Samantha A. Morris, Guo, & Zernicka-Goetz, 2012). The onset of ZGA is initiated with a minor burst of genomic DNA transcription at the one-cell stage and major burst at the 2-cell stage. Before ZGA, the embryonic development depends on maternal stores of mRNAs and proteins. With the start of the zygotic transcription, degradation of the maternal mRNA is induced, 90% are degraded when the 2-cell stage is reached (reviewed in Mihajlović & Bruce, 2017; Schultz, 1993). Nevertheless, some maternal proteins can persist until the end of the preimplantation period. Through ZGA, embryonic cells are able to adapt to environmental changes, in a plastic manner, by modified expression patterns of mRNAs and proteins in order to compensate any environmental conditions/ perturbations (reviewed in Mihajlović & Bruce, 2017).

1.1. Timeline of the preimplantation of a mouse embryo

The preimplantation stage describes the development from the zygote to the point of embryo implantation into the uterus and is determined by seven cell cycles (Figure 1). The first two cycles of cleavage division require around 20 hours while later divisions necessitate approximately 12 hours. From fertilization to a fully developed blastocyst, it takes 4.5 days, after an additional day the embryo is ready for uterine implantation. During the time of

preimplantation period, the cells undergo asynchronous cleavage divisions (whereby individual blastomere cytoplasmic volume reduces while the overall cytoplasmic volume of the embryo is not changed - reviewed in Johnson, 2009; reviewed in Mihajlović & Bruce, 2017). The embryo is surrounded by the *zona pellucida*, which is a protecting layer consisting of glycoproteins. Before uterine implantation, the embryo hatches from the *zona pellucida* to permit interaction with the endometrium (reviewed in Mihajlović & Bruce, 2017).

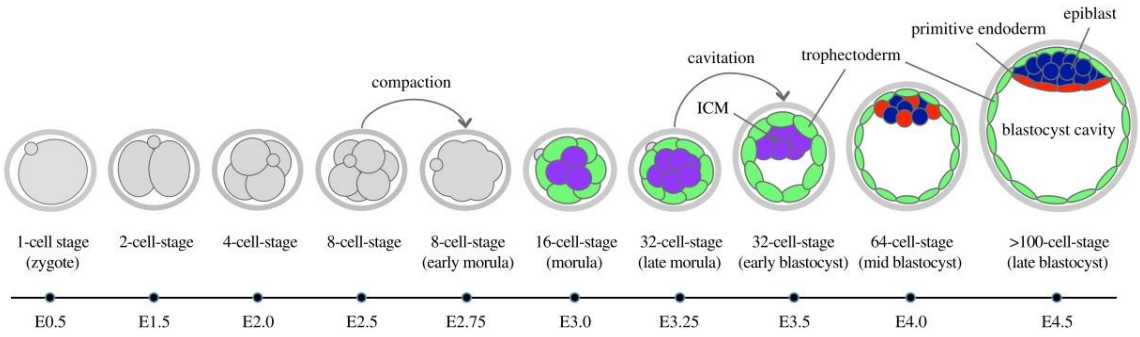

Figure 1. Timeline of the preimplantation mouse embryo development with description of the individual stages. Taken from Mihajlović & Bruce (2017).

1.2. Transitions of the preimplantation mouse embryo

Embryonic cells are considered totipotent until and including the 8-cell stage, which means every blastomere can develop to give rise to progeny cells of all three distinct blastocyst cell lineages; i.e. the trophectoderm (TE), primitive endoderm (PrE), and epiblast (EPI) (reviewed in C. Chazaud & Yamanaka, 2016). At the 8-cell stage, the first morphological changes occur in the phase of compaction. The appearances of the cells alter from obviously spherical to more flattened and with increased intercellular contacts. Microvilli are excluded from the cell – cell contact regions, as adherens junctions form, becoming limited to the contact-free, termed apical, cellular domain. A phase of intra-cellular polarization then ensues whereby specific cellular components (mainly protein factors) become asymmetrically distributed, thus contributing to the formation of molecularly distinct apical and basolateral intra-cellular domains, along the radial axis of the embryo (Figure 2). At the 32-cell stage, the so-called late morula, the embryo experiences a second morphological change referred to as cavitation (stage E3.5, Figure 1), initiating the formation of a liquid filled cavity within the embryo, often referred to as the blastocoel. At this stage, the embryo is called a blastocyst (Mihajlović & Bruce, 2017; Saiz & Plusa, 2013).

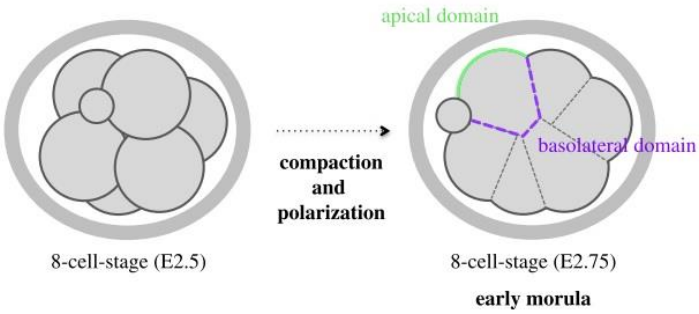

Figure 2. 8-cell stage mouse embryo undergoes compaction and intra-cellular polarization, forming apical and basolateral domains. Taken from Mihajlović & Bruce (2017).

1.3. The first cell fate decision

The first cell fate decision describes the point when blastomeres undergo spatial segregation and occurs between the 8-cell stage and the 32-cell stage. Each cell responds to its relative position in the embryo by committing to one of two fates; an apical-basolateral polarised cell positioned on the outside of the embryo will differentiate towards the TE lineage, whereas an inner apolar cell within the emerging ICM will retain pluripotency. The TE blastomeres are committed to be precursors of placental structures, the ICM gives rise to the embryo proper and its associated membranes, derived from the PrE (Sutherland, Speed, & Calarco, 1990). It is known that the spatial position and the extent of apical-basolateral polarity informs the lineage decision but is not necessarily absolute in determining the fate (reviewed in Mihajlović & Bruce, 2017). Historically, three theories have been postulated to explain the derivation of the described cell lineages: The mosaic, the positional, and the polarization model.

1.3.1. Models for the first cell fate decision

1.3.1.1. Mosaic model

It is an out-dated model that stated molecular asymmetries present throughout the zygote (and thus asymmetrically inherited in the subsequent cleavage cell divisions) instruct cells to adopt TE or ICM cell fates; therefore suggesting that cell fate is already determined in the 1-cell stage. Studies from Tarkowski & Wróblewska (1967), using disaggregated blastomeres from early stage embryo, refuted the mosaic model and instead proposed the positional model.

1.3.1.2. Positional model

The positional model argues that the position of the blastomeres in the 32-cell stage, defines the later cell fate. This model was suggested by Tarkowski & Wróblewska (1967). In their experiments, single blastomeres of 4-cell and 8-cell embryos were *in vitro* cultured for further development, eventually giving rise to blastocyst-like structures. They showed that blastomeres taken from the 4-cell stage were able to develop into morphologically normal blastocysts at high rates but the blastocysts from 8-cell stage embryos, gave rise to structures; that they termed 'false blastocysts', which at first appeared normal but lacked an ICM. The theory of Tarkowski & Wróblewska (1967) stated that the formation of a proper blastocyst is mainly due the enclosure/ encapsulation of single cells by other cells in the developing embryo. It was hypothesized that blastomeres that become altered in terms of their relative positional environment, adapt to the surroundings and thus form a specific tissue. Hillman, Sherman, & Graham (1972) tested this hypothesis by the addition of labelled single blastomeres to unlabelled embryos and proved that the labelled cells were able to adjust to their relative spatial position within the cell/ embryo cluster. In a further experiment, embryos of 4-cell and 8-cell stage were labelled and centrally or peripherally placed within the unlabelled embryos. Cells which were placed on the outside could be found contributing mostly to the TE and centrally positioned labelled cells tended to form ICM (Johnson, 2009). The positional model claims that the distinct fate of TE and ICM depends on the generation and subsequent recognition of relative cellular positional information in the developing embryo.

1.3.1.3. Polarization model

Historically, a variety of experiments (as discussed above) have verified the relationship between relative blastomere position and its subsequent cell fate, thus supporting the positional model. However, the mechanistic background for the arrangement within the cell complex, was much less understood.

In the experiments of Johnson & Ziomek (1981), the fluoresceinated ligand concanavalin A (FITC-Con A) which specifically binds to polarized surfaces, was used to visualise blastomere polarization in the developing mouse embryo. It was shown that cells become polarized, along the apical-basolateral axis, before the onset of the inner cell generation at the 8-cell stage (Johnson & Ziomek, 1981; Ziomek & Johnson, 1980). The study of Johnson & Ziomek (1981) also showed that cells can divide in two ways, in a conservative/symmetric or a differentiative/asynchronous manner (Figure 3). Conservative/symmetric means that the cell

divides equally into two outer cells at the apical-basolateral axis, hence both daughter cells maintain their polarization. By contrast, differentiative/asynchronous cells divide between the apical pole and the basolateral pole and generate an apolar inner and a polar outer cell (Bischoff, Parfitt, & Zernicka-Goetz, 2008; reviewed in Bruce & Zernicka-Goetz, 2010; Johnson & Ziomek, 1981; reviewed in Saiz & Plusa, 2013). It was thus suggested that the polarization level of a derived cell determines its cell fate.

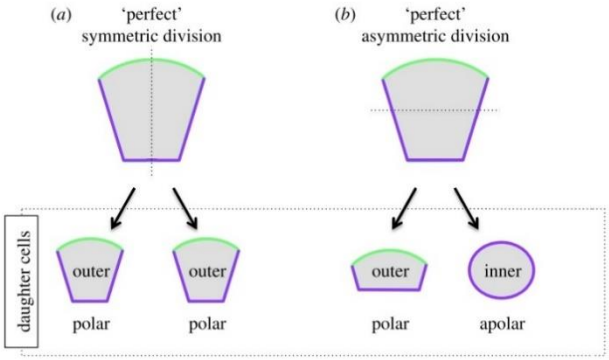

Figure 3. Scheme of polarization showing the dependence on the cleavage axis. (a) The division is symmetric, the polarization is equally passed on to the daughter cells. (b) The cell divides asymmetrically, one cell inherits all the polar parts, while the other becomes apolar. Taken from Mihajlović & Bruce (2017).

1.3.1.4. Compatibility of the positional and the polarization model

The two models suggest supposedly opposing theories of cell fate decision, but possibly the mechanism is dependent on the interplay of each. At the 16-cell stage, the constituent blastomeres of the embryo are already separated into two groups, some outer/ outward facing, the others inside the embryo. Consequently, it is of interest if the cell fate is already determined by this position or if it is still alterable. In the experiments of Suwińska, Czołowska, Ozdzeński, & Tarkowski (2008), 16-cell stage blastomeres were rearranged within the embryo and left for further development. The resultant embryos developed successfully to normal, fertile mice. However, in another experiment using 32-cell stage embryos, further development was not possible as the embryos failed to successfully implant in the uterus and thus died. These data led to the conclusion that individual blastomeres remain totipotency until the 16-cell stage and imply polarization is dependent on relative position and can be reconstructed in response to respective repositioning (Ziomek, Johnson, & Handyside, 1982).

1.3.2. Compaction on the molecular level

At the 8-cell stage, the embryo undergoes a significant change: the loosely arranged blastomeres form a compact ball. During embryo compaction, the surface area of the embryo is reduced by restricting adherens junctions to the basolateral membranes of the cells. One protein which appears to be essential for the interplay in cell contact interactions was identified by Hyafil, Morello, Babinet, & Jacob (1980); a 84,000 Dalton glycoprotein that is dependent on calcium, E-cadherin. Experiments showed, that adherens junctions were formed by release of calcium whereas depletion of calcium reduced junction formation and thus cells would become loosely arranged (reviewed in C. Chazaud & Yamanaka, 2016; Ducibella & Anderson, 1975). In further studies it was found that E-cadherin builds molecular complexes with *β-catenin* as an anchor, in order to form classical adherens junctions (Gilbert, 2014). Indeed, embryos derived from oocytes with a deficiency in maternally provided E-cadherin, or with a truncated binding part of the β-catenin allele, are not able to form adherens junctions and thus the adhesion of the cells is delayed until the translation of the embryonic transcripts begins (de Vries, 2004). Additionally, a different study performed with homozygous negative mutants for E-cadherin has demonstrated that such embryos underwent compaction but later died at implantation - such a relatively delayed impact being largely due to the presence of residual maternal E-cadherin - (Larue, Ohsugi, Hirchenhain, & Kemler, 1994). E-cadherin itself is a transmembrane protein with an extracellular domain that allows interactions with the other E-cadherins of adjacent cells. The studies of Fierro-González, White, Silva, & Plachta (2013) have shown that E-cadherins additionally contribute to the formation, during compaction, of long cellular protrusions named filopodias, that extend between adherens junctions to the apical membrane of neighbouring cells, thus, forcing the blastomeres to adopt an elongated, more compact morphology (Fierro-González *et al*., 2013; reviewed in Mihajlović & Bruce, 2017; reviewed in White & Plachta, 2015).

1.3.3. Polarization on the molecular level

Around the time of compaction, another process starts: the polarization of blastomeres along their apical-basolateral axis. Firstly, the distribution and density of microvilli within the cellular plasma-membranes are changed. A key player in controlling this concentration of microvilli to the cell-contactless apical-pole is ezrin (Louvet, Aghion, Santa-Maria, Mangeat, & Maro, 1996). Ezrin belongs to the ERM family of proteins that are involved in the formation of actin rich structures and the linkage of the actin cytoskeleton to the plasma membrane. The data of Dard, Louvet-Vallée, Santa-Maria, & Maro (2004) have shown that phosphorylation

of the T567 site in ezrin is required to stabilize microvilli at the apical pole and to degrade microvilli at the basolateral areas. This study suggested that ezrin interacts with the E-cadherin complex, but the relations between these two proteins have not yet been fully revealed. Furthermore, the mechanisms of ezrin phosphorylation and proteolytic degradation still remain unclear.

Members of the so-called '*partitioning defective*' (PAR) protein family plays an important role in polarisation of the apical-basolateral axis. The PAR proteins were identified to have regulative properties on the cleavage pattern in the nematode worm, *Caenorhabditis elegans*, during early embryogenesis. Genetic homologs of such PAR proteins are found in various organisms (Kemphues, Priess, Morton, & Cheng, 1988). In the preimplantation development of the mouse embryo, the PAR proteins play a key role in regulating the establishment and maintenance (*i.e.* defining) of the apical-basolateral polarisation axis from the 8-cell stage. Protein complexes of individual PAR factors in the mouse embryo are localised in different areas; junctional adhesion molecule A (JAM1), atypical protein kinase C (aPKC), and PAR3 become apically localised while PAR1 is situated basolateral (reviewed in Zernicka-Goetz, Morris, & Bruce, 2009). A complex of PAR3, PAR6B and aPKCs, is known to control initiation of microtubule formation at the 8-cell stage and to exclude basolateral proteins form the apical-lateral area (reviewed in Goldstein & Macara, 2007; reviewed in Yojiro Yamanaka, Ralston, Stephenson, & Rossant, 2006). Furthermore, experimental down-regulation of PAR3 and aPKC has been shown to affect the frequency of asymmetric cell divisions, whereby, for example, a lower expression of aPKC increases the frequency of observable asymmetric divisions and can promote cells to adopt an inner cell position (Plusa, 2005).

1.3.4. The first cell fate decision on the molecular level

In order to promote cell lineage segregation, transcription factors (TFs) support or suppress specific gene expression programs for each lineage. Thus, cell lineage segregation, and more specifically cell differentiation, starts with the up-regulation of lineage specific TFs and the down-regulating of other, often pluripotency related, TFs. One of the earliest known TFs promoting TE lineage is CDX2, other regulatory TFs are TEAD and EOMES (reviewed in Zernicka-Goetz *et al.*, 2009). Studies with EOMES null mutants have shown defects in proliferation of the trophoblast (Strumpf, 2005). In contrast, TFs essential for ICM differentiation are OCT4, SOX2, and NANOG. NANOG, a late acting TF, is promoted by OCT4 and SOX2. It is a member of the homeobox family of TFs and is needed for the preservation of the pluripotency and resistance against differentiation towards extraembryonic

endoderm and trophectoderm. Therefore it is a marker for the EPI lineage (Hart, Hartley, Ibrahim, & Robb, 2004).

Expression of the TE specific TF CDX2 starts at the 8-cell stage. The mRNA is asymmetrically distributed in the blastomere with the enrichment at the apical pole. Because of the asymmetrical allocation in differentially dividing cells, daughter ICM cells inherit unequal proportions of CDX2. Cells adopting an inside position have reduced levels of the pluripotency suppressing CDX2, hence express ICM promoting proteins. In the study of Strumpf (2005), homozygous *Cdx2* mutants were produced to determine the role of CDX2 in TE formation. The mutants could form a blastocoel, that continually collapsed, and the embryo failed to implant, as they could not hatch, and could not restrict OCT4 and NANOG to the blastocyst ICM. Thus, *Cdx2* is required for specification and differentiation of TE. Another study has also proposed that CDX2 might have a regulative function in cell division, demonstrating symmetric divisions to be promoted by elevated levels of CDX2, while diminished CDX2 levels resulted in higher numbers of asymmetric divisions (Jedrusik *et al*., 2008). Blij, Frum, Akyol, Fearon, & Ralston (2012) have examined a potential role for maternally provided CDX2, by means of a conditional null allele, but concluded it has no impact on the development; this is in contrast with a further study by Jedrusik, Cox, Wicher, Glover, & Zernicka-Goetz (2015), also utilising maternal-zygotic null *Cdx2* embryos (effects of this mutation could be recognized already at the morula stage).

Enhanced *Cdx2* expression is correlated with the presence of the polarised apical domain and thus regulated by a further mechanism that senses polarity and relative blastomere positioning. Relative cell position can be defined by differential activity of the Hippo-signalling pathway (defined by different proteins, like AMOT, Yes-associated transcriptional co-factor protein 1/YAP1 and transcriptional enhancer factor TEAD4) AMOT, an essential Hippo-pathway activator, binds homogenously around the plasma membrane of inner cells, coincident with sites of adherens junction formation. However, in outer cells it is restricted to the polarized apical pole of the cell, away from the adherens junction complexes found in the basolateral domains in cell-cell contact. In the inner cells, AMOT localised at the adherens junctions is activated by phosphorylation and activates, together with the help of NF2, the Hippo-effector kinase LATS1/2 kinase, which in turn phosphorylates YAP1. Due to a lack of adherens junction localisation of AMOT in outer polarised cells, YAP1 remains unphosphorylated (Wang, Huang, & Chen, 2011; Zhao *et al*., 2011). Given unphosphorylated YAP1 can enter the nucleus, and interact with TEAD4 to drive transcription of the *Cdx2* gene, an appropriate TE specific pattern of gene expression can be initiated whereas this is blocked in ICM cells,

as active Hippo-signalling ensure YAP1 remains outside the nucleus; despite TEAD4 itself being nuclear (Yagi *et al*., 2007; reviewed in Zernicka-Goetz *et al*., 2009). Interestingly, the restriction of *Sox2* TF (as a pluripotency retaining protein) gene expression to inner cells has also been shown to be dependent on active Hippo-signalling in these cells (Wicklow *et al*., 2014), although the mechanism is unknown. SOX2 itself has no regulative purpose during blastocyst formation but it plays a role in the expression of other pluripotency maintaining proteins like Nanog and OCT4. Thus, the Hippo-pathway controls the formation of both lineages TE and ICM (reviewed in C. Chazaud & Yamanaka, 2016; reviewed in Mihajlović & Bruce, 2017).

1.4. Second cell fate

In the second cell fate, the ICM segregates into two new cell lineages: the EPI and the PrE. The EPI is a progenitor lineage of the later foetus, the PrE builds the supporting tissues for the foetus, in particular the extraembryonic endoderm layers of the visceral and parietal yolk sacs (Claire Chazaud, Yamanaka, Pawson, & Rossant, 2006).

1.4.1. Second cell fate on the molecular level

The up-regulation of the transcription factor proteins GATA6, SOX17 and GATA4 induces the formation of PrE, in ICM cells in which *Nanog* expression becomes reduced. In contrast, in EPI cells *Nanog* expression is maintained and *Gata6* expression becomes down-regulated; *Sox17* and *Gata4* fail to be activated (reviewed in Zernicka-Goetz *et al*., 2009). GATA4 is also known to play a pivotal role in cardiac development as experiments with homozygous null mutants resulted in embryos that failed in the formation of heart tubes and died at an early embryonic stage (Perrino & Rockman, 2006). GATA6 is necessary in the development of the later endoderm. In experiments with a *Gata6* homozygous null mutant, embryos showed a lack of visceral endoderm (Morrisey *et al*., 1998).

1.4.2. Models for the second cell fate decision

It is still not fully understood which mechanism drives the formation of the two distinct ICM lineages. There are a few theories attempting to explain this.

1.4.2.1. Positional induction model

The positional induction model reflects a similar concept as the positional model of the first cell fate. Namely, due to relative positional differences, blastomeres lining the blastocoel have different properties than blastomeres surrounded by other blastomeres, residing deeper within the ICM. This theory suggests that the blastomeres are bipotent and the differentiation is initiated by outer signals. In experiments with immuno-surgically removed ICMs from giant blastocysts (embryos formed from three or more individual and aggregated morula staged embryos), an endoderm-like layer, the so-called primary endoderm, was established on the outside. This structure could be determined with the visceral endoderm marker alpha-fetoprotein (AFP). Furthermore, when the primary endoderm was removed, another endoderm like structure was subsequently formed, called secondary endoderm. These experiments suggest that all ICM cells are capable of forming PrE (Dziadek, 1979).

1.4.2.2. 'Salt and Pepper pattern' segregation model

This cell-sorting model states that there is inherent heterogeneity between individual ICM cells. It is known that the proteins GATA6 and NANOG are found in all cells in high concentrations from the 8/16-cell stage and this persists to the ICM cells at E3.5 stage; however, as the blastocyst matures this homogenous expression pattern changes so that individual cells exhibit either high levels of PrE specific GATA6 or EPI specific NANOG (~E4.0). It is suggested that such an expression pattern is caused by differential mRNA degradation. Furthermore, a co-regulator relationship between the two proteins appears to play a role: A higher level of NANOG protein in EPI cells suppresses *Gata6* expression and processing of fibroblast growth factor (FGF) signalling, and concurrently increases fibroblast growth factor-4 (*Fgf4*) expression. The excreted FGF4 in turn binds to the fibroblast growth receptors (FGFRs) of other cells, thus initiating up-regulation of *Gata6* and down-regulation of *Nanog* expression in the PrE precursor cells (Figure 4, A). This was shown in experiments of Krawchuk, Honma-Yamanaka, Anani, & Yamanaka (2013) and Kang, Piliszek, Artus, & Hadjantonakis (2013) where inactivation of FGF4 triggered a bias towards production of EPI cells. In contrast, elevated levels of FGF4 increases the tendency to form PrE cells (Y. Yamanaka, Lanner, & Rossant, 2010). The distribution of EPI and PrE precursor cells (~E4.0) within the ICM is depicted as a so-called 'Salt and Pepper pattern' (Figure 4, B). Due to this pattern, cell sorting must occur, whereby some inappropriately positioned PrE cells need to reach their correct position in contact to the blastocoel, and *vice-versa* in relation to EPI cells. Although the mechanism is not well understood, different factors such as TFs, proteins

important for cell polarity, cell signalling proteins or the unequal pressure of blastocoel and polar TE are suggested to play roles in this sorting process (reviewed in C. Chazaud & Yamanaka, 2016).

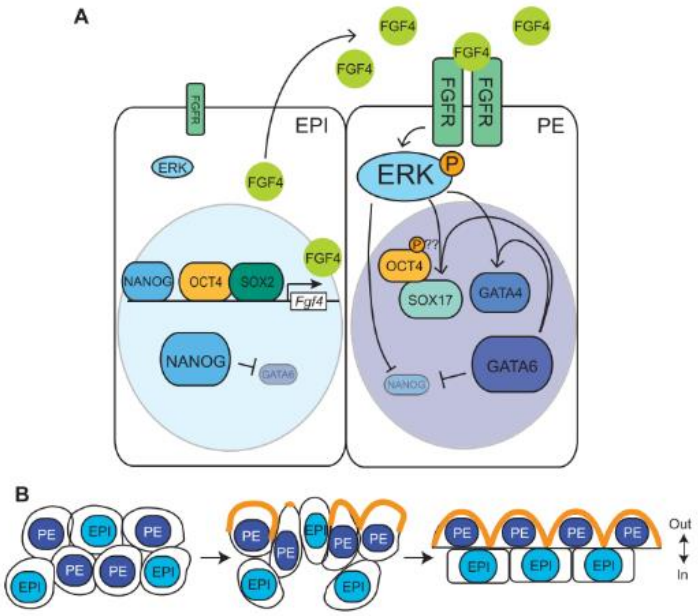

Figure 4. (A) Scheme of the regulation of the EPI/PrE (PE in the figure) formation in Salt and Pepper model. (B) Cell sorting of the randomly distributed PrE/EPI cells ('Salt and Pepper pattern'). Taken from C. Chazaud & Yamanaka (2016).

1.4.2.3. Integrated cell-fate model

An alternative hypothesis, termed the integrated cell-fate model, suggests that blastomeres of the early ICM are already biased towards the EPI or PrE cell fate, depending upon the developmental history of their predecessors. The ICM is created in two waves of asymmetric cell cleavage events (*i.e.* at the 8- to 16- and 16- to 32-cell transitions), and it was proposed that each of these divisions might give rise to differentially biased ICM cells. In an experiment with live cell imaging and cell lineage tracing of cleaving embryos, blastomeres internalised during the first wave of asymmetric division have been shown to bias towards an EPI cell fate, while inner blastomeres created during the second wave showed a bias towards the PrE lineage (S. A. Morris *et al*., 2010). Different levels of *Fgfr2* expression in inner cells derived by these two waves of division could affect blastomeres' subsequent cell fate. Indeed, experiments evoking induced and clonal overexpression of *Fgfr2* have shown a bias of derived ICM cell fates towards the PrE lineage (Samantha A. Morris, Graham, Jedrusik, & Zernicka-Goetz, 2013). Furthermore, it has been reported that inner blastomeres of the second wave exhibit higher levels of FGFR2 than blastomeres of the first wave of asymmetric cell division.

Accordingly, it appears the longer cells remain on the outside of the embryo, the more probable it is that FGFR2 expression is up-regulated and then passed on to inner cell descendants (reviewed in Leung & Zernicka-Goetz, 2015). FGF4 ligands bind to the FGFR2 receptors, thus cells with higher amounts of FGFR2 are potentially molecularly primed towards adopting a PrE lineage/ segregation fate. The mechanism underpinning such differential expressions patterns in cells contributing ICM progenitors during the first and second asymmetric divisions is still unclear; it is hypothesised that the extended exposure to the TE developing cues could guide the formation of the PrE lineage (Mihajlovic, Thamodaran, & Bruce, 2015).

It is important to note that the described models are not mutually exclusive, although they have different concepts regarding the formation of the second lineage. In the study of Mihajlovic *et al*. (2015) it was proposed that the integrated cell-fate model is not dictating the cell fate but rather guiding, and also stochastic gene expression may influence cell fate.

1.5. Relevant signalling genes for cell fate determination

Graham et al. (2014a), attempted to systematically identify genes that have an impact on lineage segregation in the preimplantation embryo. They started by performing mRNA deep sequencing of inner and outer cells isolated from 16-cell stage embryos and hypothesised that large differences in gene expression, between the two spatially distinct compartments, could reflect potentially important cell fate related genes. These data suggested the bone morphogenetic protein (BMP) signalling cascade as a possible player. This pathway is known to have regulatory properties during the early phases of post-implantation development. In the studies of Graham *et al.* (2014a) it was shown, that BMP-signalling is also a mediator for successful PrE and TE development, but not derivation of the EPI.

Besides the BMP signalling, other candidates possibly involved in cell segregation were identified. One of these proteins is the Vascular endothelial growth factor receptor 2 (VEGFR2), also known as fetal liver kinase 1 (FLK-1) or kinase insert domain protein receptor (KDR). The VEGF receptors are known to play a pivotal role in embryogenesis as they are needed in the initial formation of blood vessels (vasculogenesis) and then later during angiogenesis (the formation of blood vessels from pre-existing vessels). The VEGF receptor belongs to the receptor tyrosine kinase (RTK) superfamily, that also includes FGFRs and platelet derived growth factor receptors (PDGFRs) (reviewed in Olsson, Dimberg, Kreuger, & Claesson-Welsh, 2006). Members of the RTK superfamily are cell membrane bound

receptors with an intra-cellular tyrosine kinase domain. The RTK receptors are activated by ligand binding on the extracellular surface, which causes a conformational change, that then induces the phosphorylation of substrate (including auto-phosphorylation) tyrosine residue (Alberts, Johnson, Lewis, Raff, Roberts, Walter Lefers, 2009). The VEGFRA/VEGFR2 signalling complex is involved in endothelial cell proliferation, survival, migration, and formation of new blood vessels. In the experiments of Graham *et al.* (2014b) (described above) the mRNA encoding VEGFR2 was found enriched in the inner cell population versus the outer cells; thus, indicating the possibility VEGFR-signalling may be involved in the segregation of either TE and ICM cell fates, or potentially/ additionally PrE and EPI fate within the ICM.

Accordingly, in the experiments presented here, we wanted to investigate for the presence of a potential cell-fate role of VEGFR2 activation during the lineage segregations observed during the development of preimplantation stage mouse embryo. This was achieved by the suppression of VEGFR2 activity using the potent and selective pharmacological inhibitor, Vandetanib (Van).

2. AIMS

The aim of this thesis was to assay for functional evidence of active VEGF-signalling, via the VEGFR2, in directing derivation of cells of the preimplantation stage embryo towards one or more of the three blastocyst stage cell lineages (TE, PrE, or EPI), using a pharmacological approach of VEGFR2 activity blockade, during *in vitro* culture.

3. Materials and Methods

3.1. Embryo Collection

The experiments were performed with 9-week old F1 hybrid female mice (CBA/W x C57Bl6). Females were super-ovulated by intra-peritoneal injection of 10 IU Pregnant Mare Serum Gonadotropin (PMSG; Sigma-Aldrich) followed by 10 IU human chorionic gonadotropin (hCG; Sigma-Aldrich) administered 48 hours after PMSG injection, and mated with F1 males. 16 hours later, successful fertilization was determined by identification of the characteristic vaginal plug and female were separated from male mice. 1.5 days after fertilization (approximately 44 hours after hCG administration), the embryos reached the embryonic day 1.5 (E1.5, 2-cell stage). At this point, the mice were killed by cervical dislocation. The oviduct was dissected and immersed in M2 solution in a 1.5mL microtube for transportation. The oviduct was then cut, the embryos were recovered into M2 medium containing 4 mg/mL BSA and washed through M2 drops covered by mineral oil (Irvine Scientific) on the culture dish.

3.2. Mouse embryo *in vitro* culture

For embryo cultivation, Embryo-Max KSOM growth medium was used (Millipore). KSOM drops (~10µL) were pipetted on tissue culture dishes (35 x 10mm) and covered by mineral oil (Irvine Scientific). Embryos were first washed through KSOM drops and then cultured in KSOM under mineral oil in a 5% CO_2 containing atmosphere at 37°C.

For VEGFR2 inhibition, the chemical inhibitor Vandetanib (diluted in DMSO, Selleckchem) was used, at concentrations of 4nM, 40nM, 400nM, 20µM, and 50µM in KSOM. Control embryos were cultured in corresponding volume of DMSO (Sigma-Aldrich) vehicle, in KSOM. The inhibition was performed either immediately from 2-cell stage (E1.5) or at 8-cell stage (E2.5) until early or late blastocyst stage (E3.5 or E4.5, respectively) (Nagy, Gertsenstein, Vintersten, & Behringer, 2003).

3.3. Fixation

When the embryos reached the required developmental stage, the *zona pellucida* was removed by using acid Tyrode's solution (Sigma). Dishes with M2 and acid Tyrode's solution drops were prepared. The prepared dishes and additional tubes filled with M2 and acid Tyrode's solution were kept in the incubator at 37°C for 20 minutes. To remove the *zona pellucida*, the embryos were transferred into the acid Tyrode's solution drops and incubated there until the

zona pellucida was dissolved. The removal was judged visually: when the *zona pellucida* could not be recognized, the embryos were washed in M2 media. Embryos were then fixed in a 96-well plate, filled with 100µL agar, covered by the 4% paraformaldehyde (PFA; Santa Cruz Biotechnology) fixative solution and overlaid with mineral oil (Irvine Scientific). After 20 minutes incubation in 4% PFA, at room temperature, the embryos were twice washed in 100µL phosphate-buffered saline Tween-20 (PBST) and incubated in third PBST wash (100µL) drop for 20 minutes, at room temperature.

3.4. Permeabilisation and immuno-fluorescent staining

Permeabilisation of the cell membranes was performed in 200µL 0.5% Triton-X100 (Sigma-Aldrich) in 1x PBS in the wells of a 96-well tissue culture plate; the embryos were incubated for 20 minutes at room temperature. Afterwards, the embryos were twice briefly washed, in a similar manner, in PBST and then left in a third PBST wash for 20 minutes at room temperature. Embryos were then transferred into a blocking solution consisting of 3% bovine serum albumin (BSA) in PBST and were incubated for a further 30 minutes at 4°C. For the fluorescent immuno-staining of CDX2, GATA4, cleaved CASPASE 3, and NANOG proteins, the embryos were immersed in the primary antibodies (anti-CDX2, Biogenex-Baria, cat. no. MU392A-UC, raised in mouse; anti-GATA4, Santa Cruz, cat. no. sc-25310 raised in mouse; anti-cleaved CASPASE 3, CST, cat. no. 9661, raised in rabbit and anti-NANOG, Abcam, cat. no. ab80892, raised in rabbit) diluted in BSA at 1:200 each and kept overnight at 4°C. Next morning, the embryos were washed twice in PBST and incubated in third PBST wash for 20 minutes at room temperature, followed by incubation in BSA block for 30 minutes at 4°C. Afterwards, the embryos were transferred into a well containing diluted secondary antibodies and Vectashield solution containing DAPI for DNA staining in BSA. The individual antibodies and Vectashield were obtained from the following suppliers and used at the following dilutions (in BSA): Alexa Fluor 647-conjugated anti-mouse antibody raised in donkey (diluted 1:500 in BSA, Jackson Immuno Research Inc., cat. no. 715605150), Alexa Fluor 488-conjugated anti-rabbit antibody raised in goat (diluted 1:250 in BSA, Life Technologies, cat. no. 1756599), and Vectashield (diluted 1:100 in BSA, Vector Laboratories). The embryos were left in the secondary antibody staining solution for 1 hour, at 4°C, followed by washing two times in PBST. At the third washing step, rhodamine phalloidin solution (diluted 1:100 in PBST, Invitrogen, cat. no. R415) was added to PBST, in order to stain cortical F-ACTIN (i.e. cytoplasmic membranes). The embryos were incubated

in this terminal solution for 20 minutes at room temperature, before being transferred to PSBT drops for confocal microscopic analysis.

3.5. Cell imaging, analysis, and counting

Embryos were scanned using an inverted laser scanning confocal microscope (Olympus FluoView TM1000 IX-80) in small PBST drops on a plate containing a glass microscope cover slip base (Matek). For visualisation of the immuno-fluorescently stained proteins and DNA, the samples were excited at 405nm (DNA), 488nm (NANOG, cleaved CASPASE 3), and 647nm (CDX2, GATA4), and each embryo was scanned in its entirety as a series of 2µm thick z-sections. Analyses of the images was performed within the Olympus FluoView V4.1a Viewer (Olympus) software. Cells of the most outer layer and inner cells were analysed separately, the numbers of stained cells were determined (Figure 5). Also, the number of cells with multiple stains was detected. For better recognition of discrete cells, DNA staining was used. Cells undergoing mitosis were counted as one cell except the fate of the daughter cells was clear, then they were assigned to the respective group.

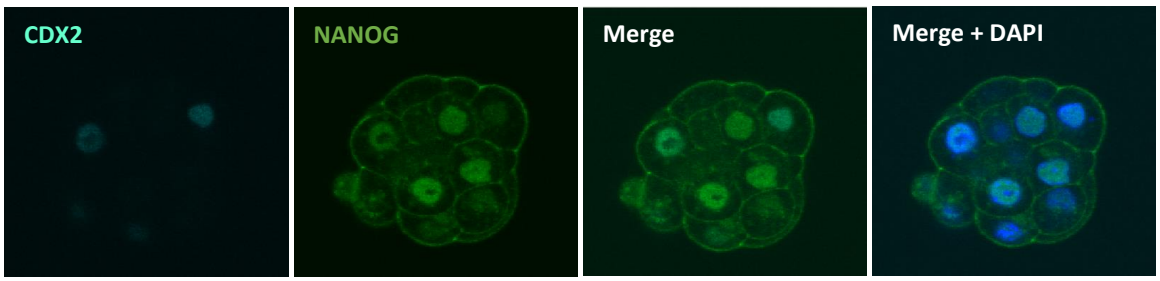

Figure 5. Example for confocal microscopy analysis of CDX2 (turquoise) and NANOG (green) proteins in the control group of experiment 1 at E3.5 stage. Merge shows a combined image of CDX2 and NANOG immuno-fluorescent staining. Counterstaining of DNA was performed using DAPI (blue – in second merge).

4. RESULTS AND DISCUSSION

We aimed to determine if there was a functional cell fate related role for active/ functional VEGFR2 during mouse preimplantation embryonic development. To achieve this aim, we blocked the signalling cascade by inactivation of VEGFR2 protein using an appropriate and specific chemical inhibitor called Vandetanib, added to the *in vitro* culture medium and subsequently analysed the impact on the derivation of individual cell lineages by the blastocyst stage. Categorisation of blastomeres into the blastocyst cell lineages was performed using immuno-fluorescence staining with antibodies that specifically recognise expressed cell lineage marker proteins (i.e. NANOG for ICM and EPI, CDX2 for TE, and GATA4 for PrE), In addition, the nuclei were stained with DAPI in order to determine the total number of cells, and the cytoplasmatic membranes (i.e. cortical F-ACTIN) were stained with rhodamine phalloidin, allowing the interpretation of blastomere spatial position within the cell cluster and subsequent categorisation into outer and inner cell compartments of the embryo. To assess the effect of VEGFR2 inhibition, we compared the numbers of the inner versus outer cells, and of cells marked by individual cell lineage markers between the treated and the control groups. The significance of the identified differences was tested using a two-tailed unpaired t-test; p-values < 0.005 were defined as 'significant' changes, p-values < 0.05 were set as 'potentially significant' results.

4.1. Effects of VEGFR2 inhibition on the first cell fate decision

The first cell fate decision marks the segregation of lineages towards TE and ICM. At E3.5, the blastomeres should be specified to either of the cell lineages and express appropriate lineage markers. Outer cells should be specified to TE cell lineage and express the differentiating transcription factor marker CDX2, while inner cells are specified to ICM and express the pluripotency marker NANOG. To analyse the effect of VEGFR2 inhibition on the segregation of these two lineages, we immuno-fluorescently stained embryos with antibodies against the ICM marker, NANOG, and TE marker, CDX2, and counted the average numbers of blastomeres expressing only NANOG (ICM cell), only CDX2 (TE cells), both, or neither. The presence of both CDX2 and NANOG in the same blastomere suggests a failure of an individual blastomere to specify to either of the cell lineages, and the higher frequency of such blastomere observed in the Vandetanib treated group (see below) compared to the control group could indicate a delay in the development.

4.1.1. Experiment 1 – employing 20µM Vandetanib from E1.5 to E3.5

In the first experiment, a concentration of 20µM of Vandetanib was employed. The inhibitor was added to the culture media at E1.5 immediately after dissection. To analyse the effect on the first cell fate decision, the embryos were cultured until E3.5 (Figure 6).

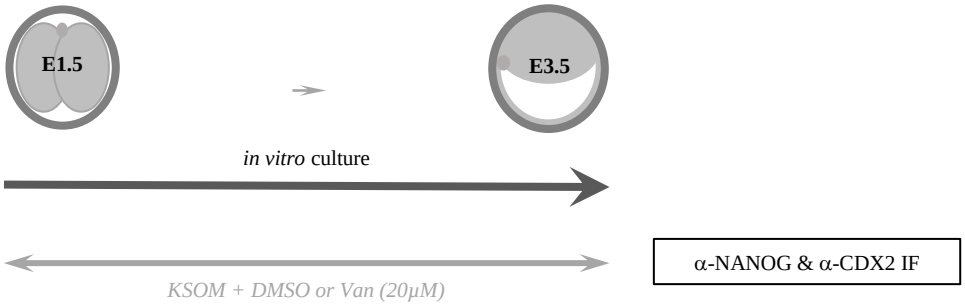

Figure 6. Schematic visualisation of the experiment 1. Embryos were treated with inhibitor from 2-cell stage (E1.5) and cultured in vitro until 32-cell stage (E3.5), fixed, and assayed for total and lineage specific cell numbers.

The overall results of the first experiment are shown in (Table 1). No significant or potentially significant difference was observed in the total number of cells, and also the counts of both inner and outer cells were similar to the values of the control group (Figure 7). In contrast, the comparison of the numbers of cell lineage-specific cells showed potentially significant differences. In outer cells, the number of blastomeres exhibiting positive staining for CDX2 alone was decreased by Vandetanib treatment (4.0 ± 1.6 versus 8.4 ± 1.3, respectively) while the number of blastomeres presenting with double staining of CDX2 and NANOG was increased (12.2 ± 1.9 versus 7.4 ± 0.8, respectively - Figure 8). A similar trend was observed in inner cells, as treated embryos also showed increased numbers of unspecified blastomeres with double positive staining (Figure 9, 10, & 11). These results suggest VEGFR2 inhibition at 20µ exhibited a modest effect on cell lineage segregation in both the TE and ICM, with the number of unspecified cells still expressing both CDX2 and NANOG markers was increased in each spatial domain (i.e. outer versus inner). Moreover, as overall cell number and the number of outer and inner cells was not changed, the results indicate VEGFR2 inhibited embryos (20µM) developed in step/stage with controls, suggesting the reason for increased number of unspecified cells is not due to an overall lag in development caused by the treatment. Interestingly, the number of ICM cells that did not stain for either lineage marker was found to be decreased in a potentially significant manner by VEGFR2 inhibition (0.3 ± 0.2 versus 1.7 ± 0.4). The reasons for this are unclear but may reflect some cells in control

already down-regulating Nanog expression as they begin specifying PrE differentiation in a manner that has not yet been initiated in the Vandetanib treated group.

		Outer Cells				
	Total Cells (all)	**Total Cells**	**Cdx2**	**Nanog**	**Cdx2 + Nanog**	**no staining**
DMSO	30.7 (1)	19.5 (0.9)	8.4 (1.3)	1.6 (0.4)	7.4 (0.8)	2.1 (0.4)
Vandetanib (20µM)	30.1 (1.2)	19.2 (1.2)	4 (1.6)	2.1 (1.6)	12.2 (1.9)	0.9 (0.4)
p-value[1]	7.31E-01	8.69E-01	4.89E-02*	7.05E-01	1.15E-02*	1.04E-01

	Inner Cells				
	Total Cells	**Cdx2**	**Nanog**	**Cdx2 + Nanog**	**no staining**
DMSO	11.2 (0.4)	0.5 (0.2)	7.7 (0.5)	1.3 (0.3)	1.7 (0.4)
Vandetanib (20µM)	10.9 (0.7)	1.7 (0.9)	5.6 (1.4)	3.3 (1)	0.3 (0.2)
p-value[1]	6.86E-01	1.13E-01	9.81E-02	1.64E-02*	2.11E-02*

Table 1. Experiment 1. Average (±SEM) values of total cells and outer and inner cells of DMSO control group (n=19) and 20µM Vandetanib group (n=9). The embryos were cultured from E1.5 to E3.5 in KSOM medium with DMSO (control group) or Vandetanib (experimental group). Outer and inner cells, judge by their relative spatial position within the embryo are categorised as staining positive for CDX2 alone or NANOG alone, respectively; double stained cells (CDX2 + NANOG) and cells with no staining (no staining) are also shown. [1]Potentially significant (*) and significant (**) differences between the groups are highlighted; two-tailed unpaired t-test, p-values < 0.05 and < 0.005, respectively.

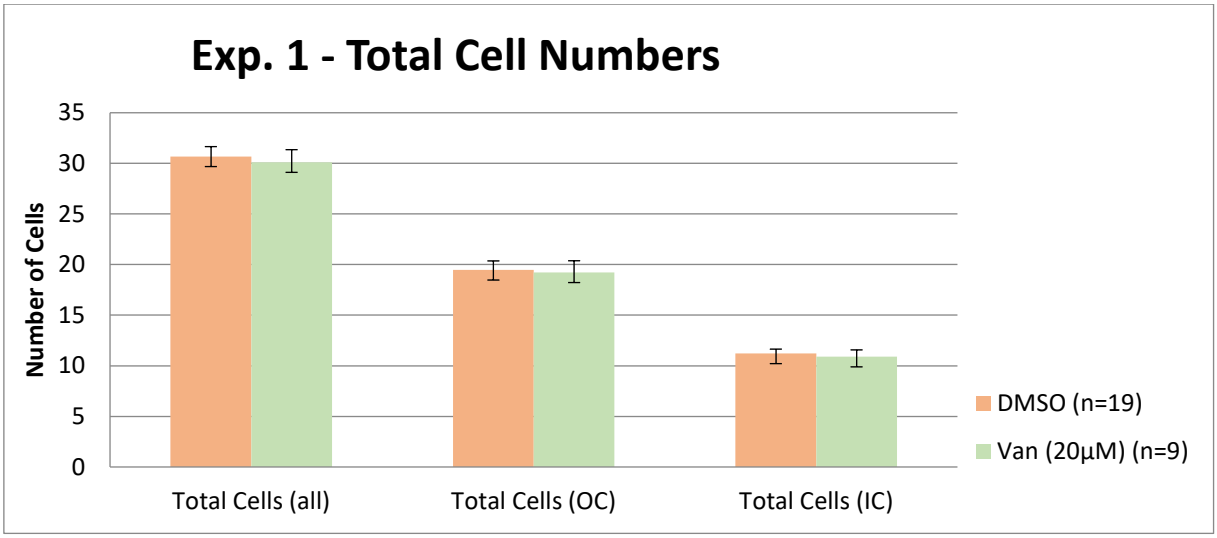

Figure 7. Average numbers of cells observed in the control group (DMSO) and the VEGFR2 inhibited group (Van), from experiment 1 (see also Table 1); plus either DMSO or Vandetanib (20µM) from E1.5 – E3.5. Comparison of the total numbers of cells as well as of inner (IC) and outer (OC) cells at the E3.5.

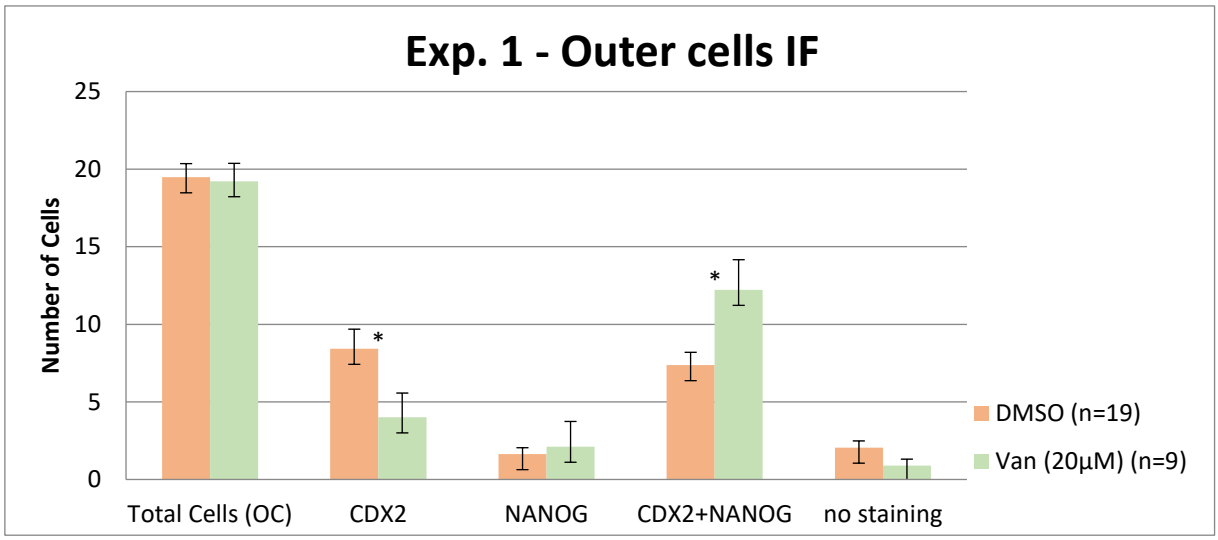

Figure 8. Average number of outer cells observed in the control group (DMSO) and inhibitor group (Van), from experiment 1; including a comparison of expression distribution of the TE marker, CDX2 and the EPI marker, NANOG. Potentially significant (*) and significant (**) differences between the groups are highlighted; two-tailed unpaired t-test, p-values < 0.05 and < 0.005, respectively.

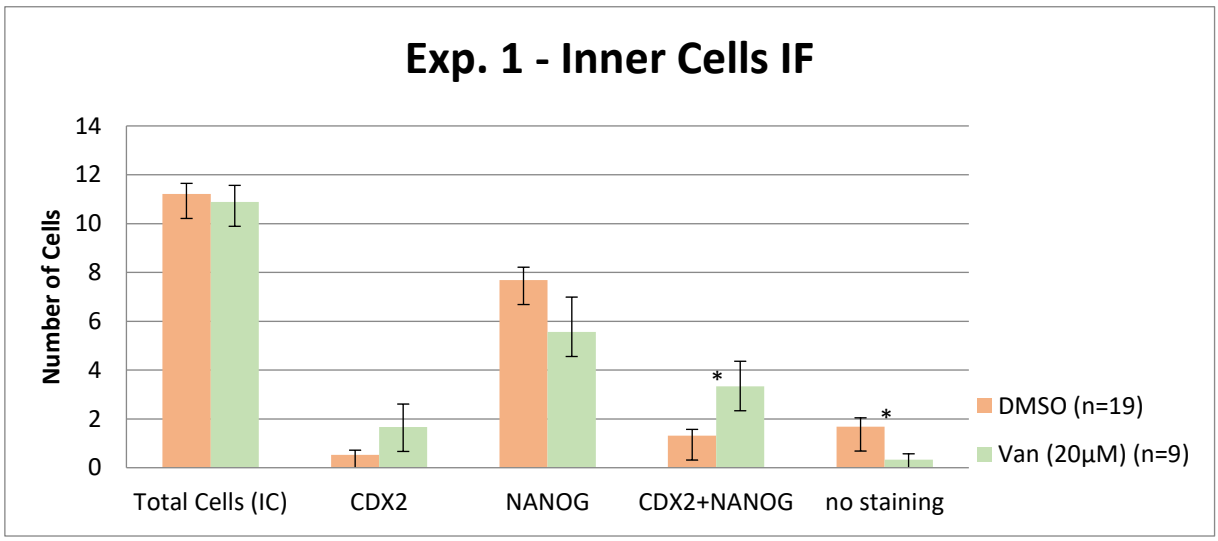

Figure 9. Average number of inner cells observed in the control group (DMSO) and inhibitor group (Van), from experiment 1; including a comparison of expression distribution of the TE marker, CDX2 and the EPI marker, NANOG. Potentially significant (*) and significant (**) differences between the groups are highlighted; two-tailed unpaired t-test, p-values < 0.05 and < 0.005, respectively.

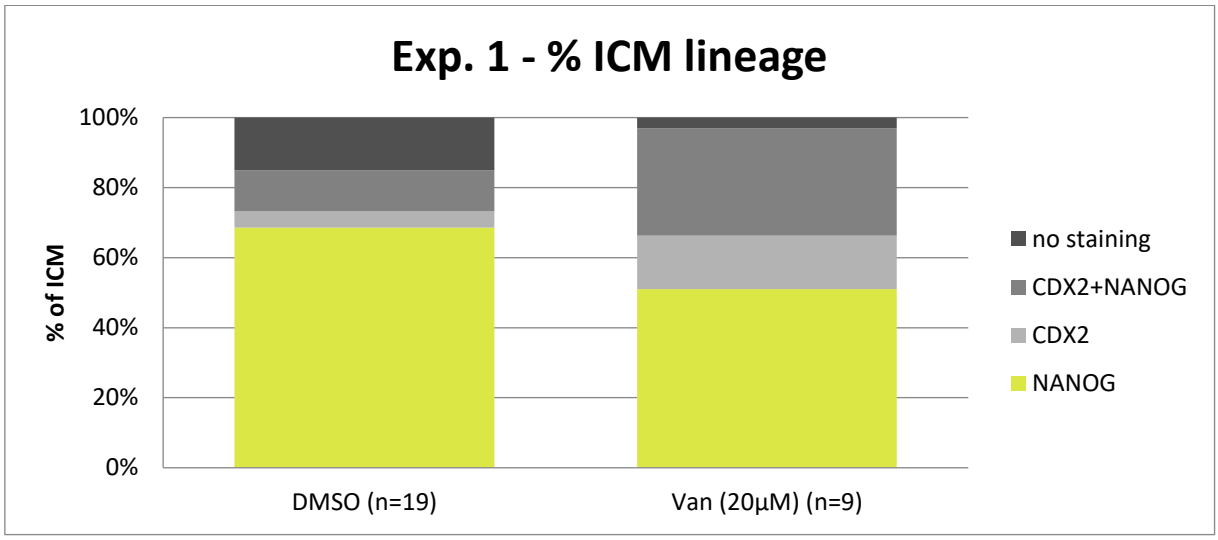

Figure 10. Average percentages of ICM assayed cells positively staining for examined lineage markers (or not) in relation to experiment 1.

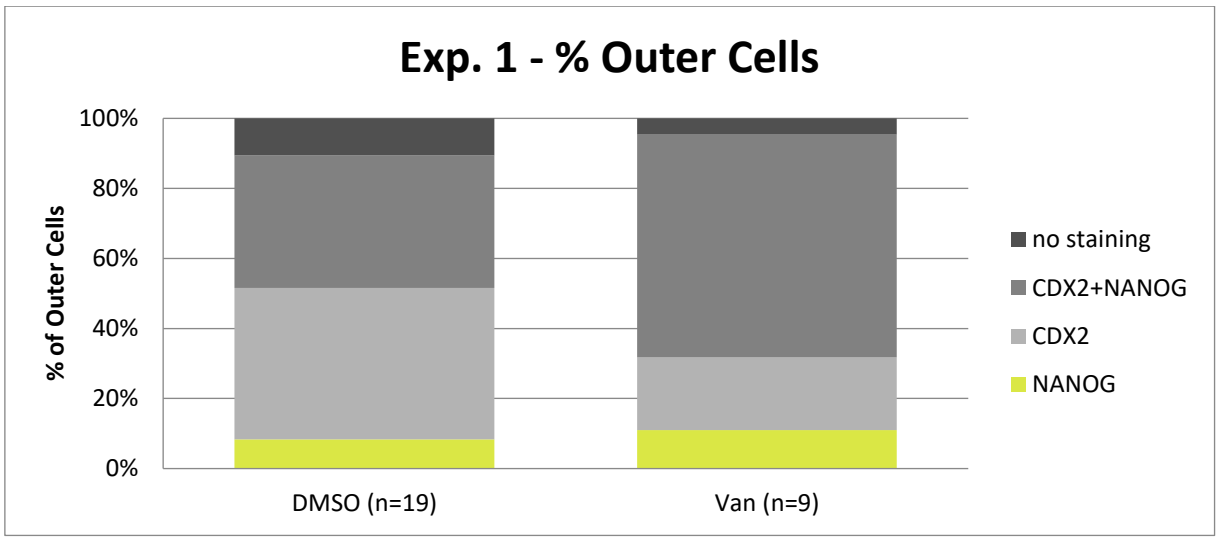

Figure 11. Average percentages of assayed outer cells positively staining for examined lineage markers (or not) in relation to experiment 1.

4.1.2. Experiment 2 – employing 20µM Vandetanib from E2.5 to E3.5

In the second experiment, in an attempt to more precisely determine the temporal sensitivity window of VEGFR2 inhibition sensitivity, we restricted the administration of Vandetanib to the *in vitro* culture to E2.5 (8-cell stage) time-point (rather than from E1.5/ 2-cell stage – see experiment 1 above). Therefore, all embryos were cultured from the 2-cell (E1.5) to 8-cell stage (E2.5) in KSOM medium, after which they were transferred into KSOM medium containing either DMSO or the inhibitor Vandetanib (20µM), before being further cultured until E3.5 when they were fixed and analysed as before (Figure 12).

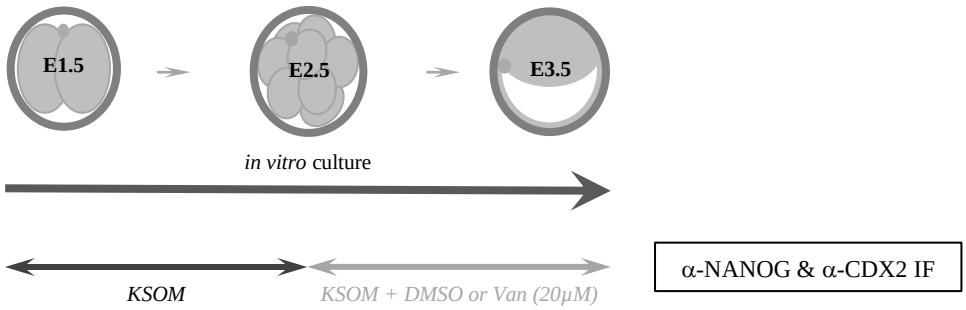

Figure 12. Schematic visualisation of the experiment 2. 2-cell stage (E1.5) embryos were cultured in KSOM media until the 8-cell stage (E2.5), then they were treated with DMSO or inhibitor and cultured in vitro until 32-cell stage (E3.5), fixed, and assayed for total and lineage specific cell numbers.

A comparison of the total cell numbers displays a significant decrease in the VEGFR2 inhibited group compared to the control embryos; 21.2 ± 1.7 versus 29.4 ± 1.0, respectively (Table 2 and Figure 13). The evaluation of average cell contributions to the specific cell lineage categories, both in inner and outer cell populations, also showed a similar trend, each classified as potentially significant (Table 2 and Figure 14 & 15). However, there were two notable exceptions. The first related to cells solely staining for CDX2 in inner cells, which were negligible in both conditions. The second related to the number of solely NANOG positive cells in the outer cell cluster. Such cells were over-represented, in a potentially significant manner, after Vandetanib treatment (3.8 ± 0.8 versus, 1.4 ± 0.7). Interestingly and in contrast to experiment 1 (administering Vandetanib from the E1.5/ 2-cell stage), no increase in double positive (CDX2/ NANOG) unspecified cells was at all observed; conversely a potentially significant reduction in their appearance was recorded (7.3 ± 1.4 versus 12.3 ± 1.2).

The comparison of the different lineages as proportions of ICM showed little differences in control and experimental group (Figure 16 & 17). While experiment 1 showed delayed specification in the inhibited embryos, in the experiment 2 the embryos appeared delayed in their overall development, as demonstrated by the lower total cell number; although it could also be possible that enhanced cell death in the VEGFR2 treated group could account for the reduced overall number of cells.

One possible explanation of the observed differences in total and lineage specific cell numbers (importantly and specifically in the numbers of unspecified cell) observed between experiments 1 and 2 would seem to relate to the developmental timing of Vandetanib inhibitor administration. It is possible, this could reflect some intrinsic biological explanation, or it could also be technical in nature. This is because in the first experiment, the inhibitor being

given at E1.5 may have become partially degraded/ inactivated and therefore become less potent by the time the embryos reached the 8-cell (E2.5) stage; i.e. the stage from which the second experimental inhibition was initiated and from which embryos exhibited a marked VEGFR2 inhibition sensitivity (using the same concentration of Vandetanib) in terms of cell numbers. Therefore, the effect of the inhibitor in experiment 1 may not have been as potent in this sensitive window, as it was in the experiment 2.

		Outer Cells				
	Total Cells (all)	**Total Cells**	**Cdx2**	**Nanog**	**Cdx2 + Nanog**	**no staining**
DMSO	29.4 (1)	19.7 (0.7)	4.3 (0.9)	1.4 (0.7)	12.3 (1.2)	1.8 (0.6)
Vandetanib (20µM)	21.2 (1.7)	15.7 (0.8)	1.9 (0.5)	3.8 (0.8)	7.3 (1.4)	2.7 (0.6)
p-value[1]	4.65E-04**	1.09E-03**	1.34E-02*	2.57E-02*	1.52E-02*	3.10E-01

	Inner Cells				
	Total Cells	**Cdx2**	**Nanog**	**Cdx2 + Nanog**	**no staining**
DMSO	0.5 (0)	0.1 (0)	0.5 (0)	0.4 (0)	0.4 (0)
Vandetanib (20µM)	2 (0)	0 (0)	2 (0)	0 (0)	0 (0)
p-value[1]	1.24E-03**	2.04E-01	2.41E-02*	6.98E-02	3.74E-02*

Table 2. Values of Experiment 2. Average (±SEM) values of total cells and outer and inner cells of DMSO control group (n=17) and 20µM Vandetanib group (n=23). The embryos were cultured from E2.5 to E3.5 in KSOM media with DMSO (control group) or Vandetanib (experimental group). Outer and inner cells judge by their relative spatial position within the embryo are categorised as staining positive for CDX2 alone or NANOG alone, respectively; double stained cells (CDX2 + NANOG) and cells with no staining (no staining) are also shown .[1]Potentially significant (*) and significant (**) differences between the groups are highlighted; two-tailed unpaired t-test, p-values < 0.05 and < 0.005, respectively.

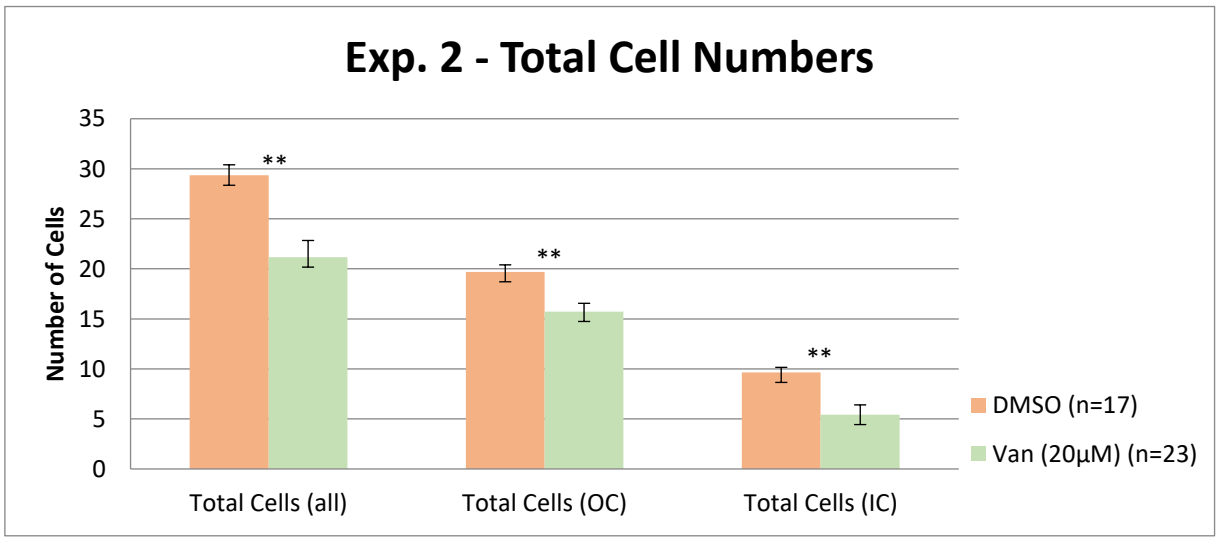

Figure 13. Average numbers of cells observed in the control group (DMSO) and the VEGFR2 inhibited group (Van), from experiment 1 (see also Table 2); plus either DMSO or Vandetanib (20 M) from E2.5 – E3.5. Comparison of the total numbers of cells as well as of inner (IC) and outer (OC) cells at the E3.5.

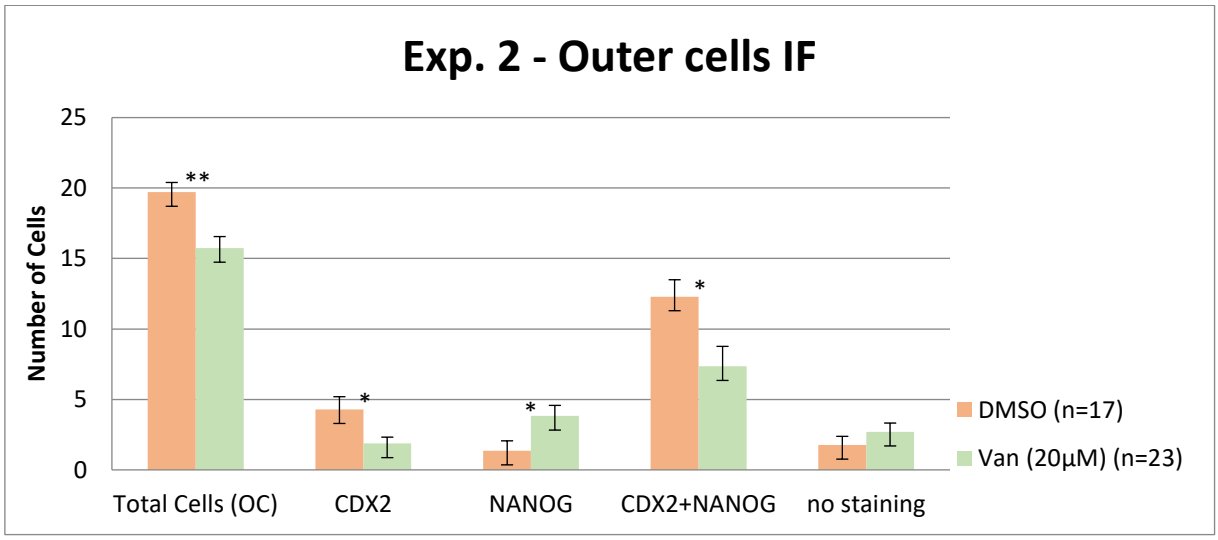

Figure 14. Average number of outer cells observed in the control group (DMSO) and inhibitor group (Van), from experiment 2; including a comparison of expression distribution of the TE marker, CDX2 and the EPI marker, NANOG. Potentially significant (*) and significant (**) differences between the groups are highlighted; two-tailed unpaired t-test, p-values < 0.05 and < 0.005, respectively.

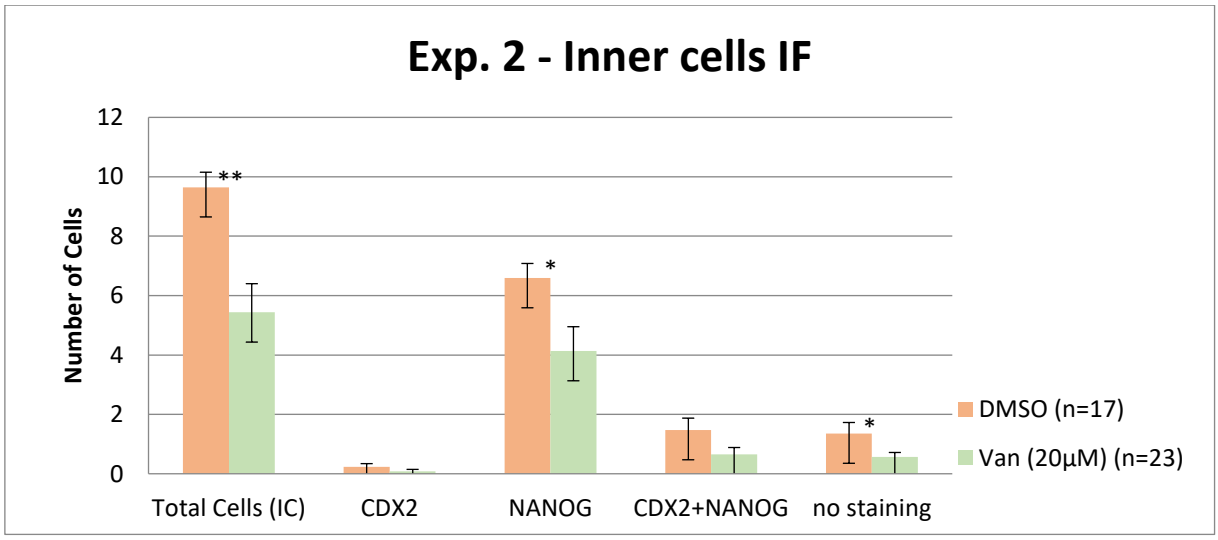

Figure 15. Average number of inner cells observed in the control group (DMSO) and inhibitor group (Van), from experiment 2; including a comparison of expression distribution of the TE marker, CDX2 and the EPI marker, NANOG. Potentially significant (*) and significant (**) differences between the groups are highlighted; two-tailed unpaired t-test, p-values < 0.05 and < 0.005, respectively.

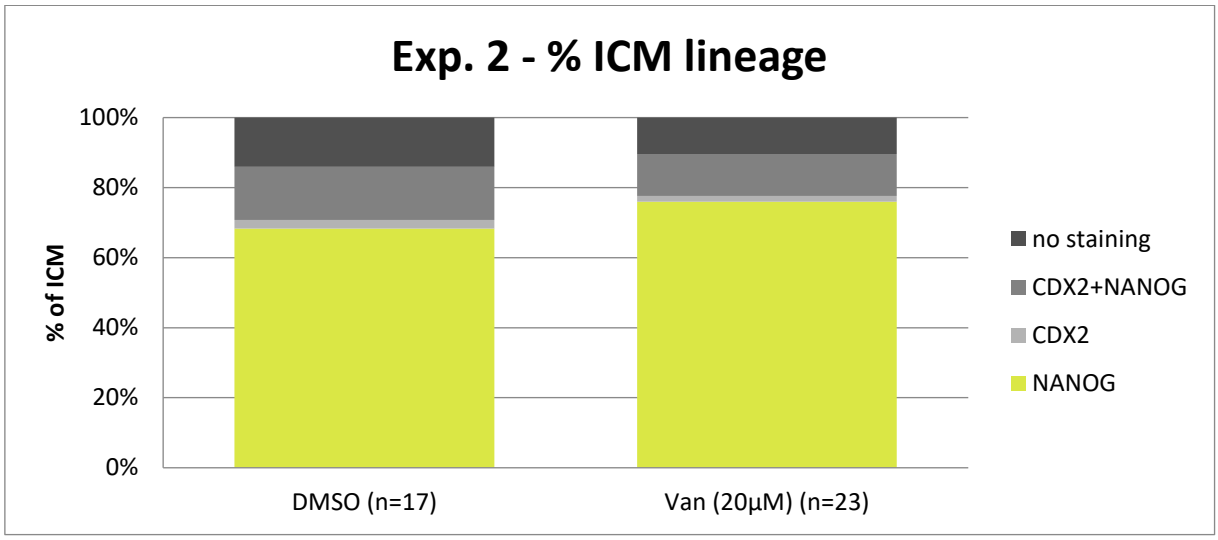

Figure 16. Average percentages of ICM assayed cells positively staining for examined lineage markers (or not) in relation to experiment 2.

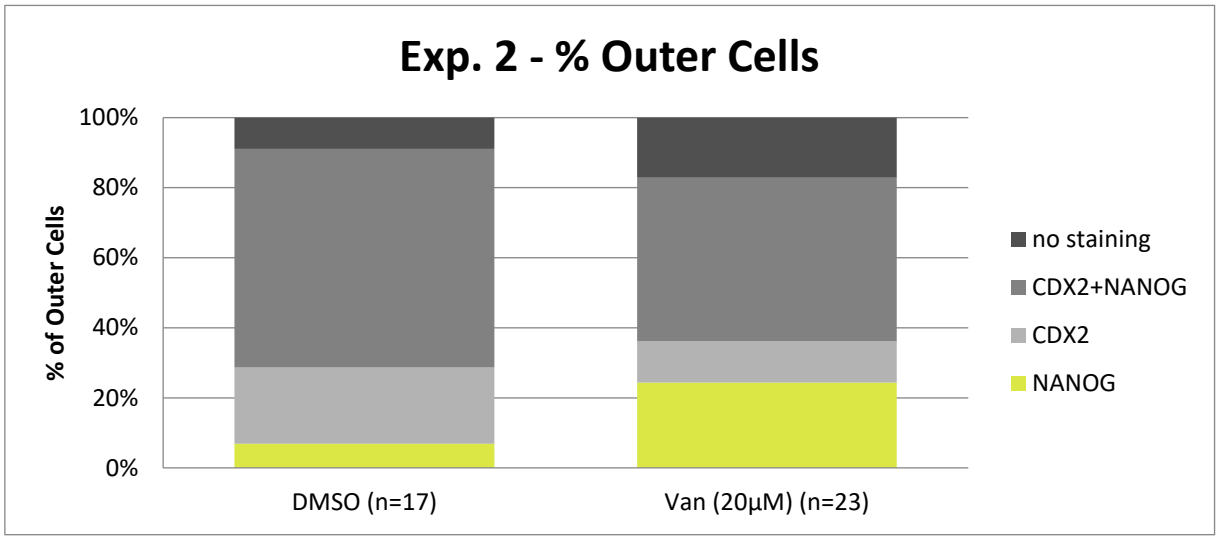

Figure 17. Average percentages of assayed outer cells positively staining for examined lineage markers (or not) in relation to experiment 2.

4.1.3. Experiment 3 – employing 50µM Vandetanib from E2.5 to E3.5

To determine whether a higher concentration of Vandetanib will lead to a more profound phenotype, we repeated experiment 2 with an increased concentration of Vandetanib inhibitor - 50µM (Figure 18).

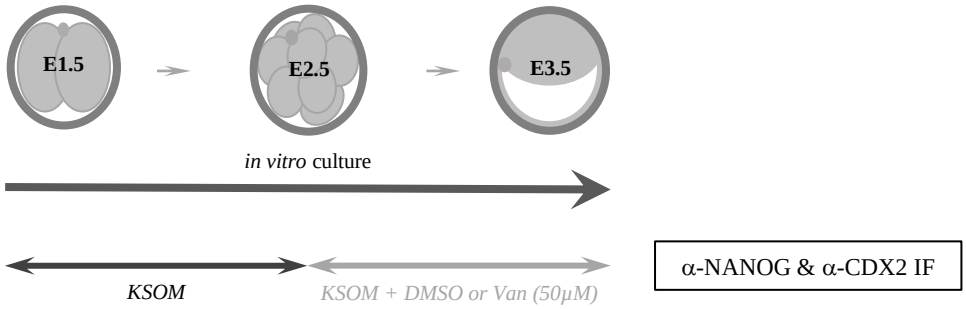

Figure 18. Schematic visualisation of the experiment 3. 2-cell stage (E1.5) embryos were cultured in KSOM media until the 8-cell stage (E2.5), then they were treated with DMSO or inhibitor and cultured in vitro until 32-cell stage (E3.5), fixed, and assayed for total and lineage specific cell numbers.

The data showed a strong developmental suppression of the treated group (Table3, and Figure18, 21, & 22). All lineage markers showed an equal trend, as the observed average cell numbers were reduced (Figure 19 & 20). Furthermore, it was noted that the morphological appearance of some cells in VEGFR2 treated (50µM) embryos was atypical compared to those observed in the control treated embryo group; indeed closer confocal microscopic inspection heavily suggested these cells had died. These results suggest that Vandetanib is lethal to the embryonic cells at the higher (50µM) concentration used. It is not possible to ascertain if this effect is the consequence of specific and strong inhibition of VEGFR2 pathway or is acting through non-specific targets.

	Total Cells	Outer Cells				
	(all)	Total Cells	Cdx2	Nanog	Cdx2 + Nanog	no staining
DMSO	32 (1)	21.1 (0.7)	6.9 (1)	2 (0.6)	10.5 (1.1)	1.6 (0.3)
Vandetanib (20µM)	13.9 (0.4)	12.3 (0.3)	0.7 (0.3)	5.2 (0.6)	1.8 (0.4)	4.7 (0.7)
p-value[1]	1.48E-26**	7.91E-17**	1.14E-08**	6.37E-04**	6.77E-12**	2.43E-04**

	Inner Cells				
	Total Cells	Cdx2	Nanog	Cdx2 + Nanog	no staining
DMSO	10.9 (0.5)	0.5 (0.4)	7.7 (0.6)	1.6 (0.3)	1.2 (0.3)
Vandetanib (20µM)	1.6 (0.2)	0 (0)	0.9 (0.2)	0.1 (0.1)	0.5 (0.1)
p-value[1]	4.27E-27**	1.52E-01	1.56E-17**	1.12E-06**	4.42E-02*

Table 3. Values of Experiment 3. Average (±SEM) values of total cells and outer and inner cells of DMSO control group (n=28) and 50µM Vandetanib group (n=35). The embryos were cultured from E2.5 to E3.5 in KSOM media with DMSO (control group) or Vandetanib (experimental group). Outer and inner cells judge by their relative spatial position within the embryo are categorised as staining positive for CDX2 alone or NANOG alone, respectively; double stained cells (CDX2 + NANOG) and cells with no staining (no staining) are also shown. [1]Potentially significant (*) and significant (**) differences between the groups are highlighted; two-tailed unpaired t-test, p-values < 0.05 and < 0.005, respectively.

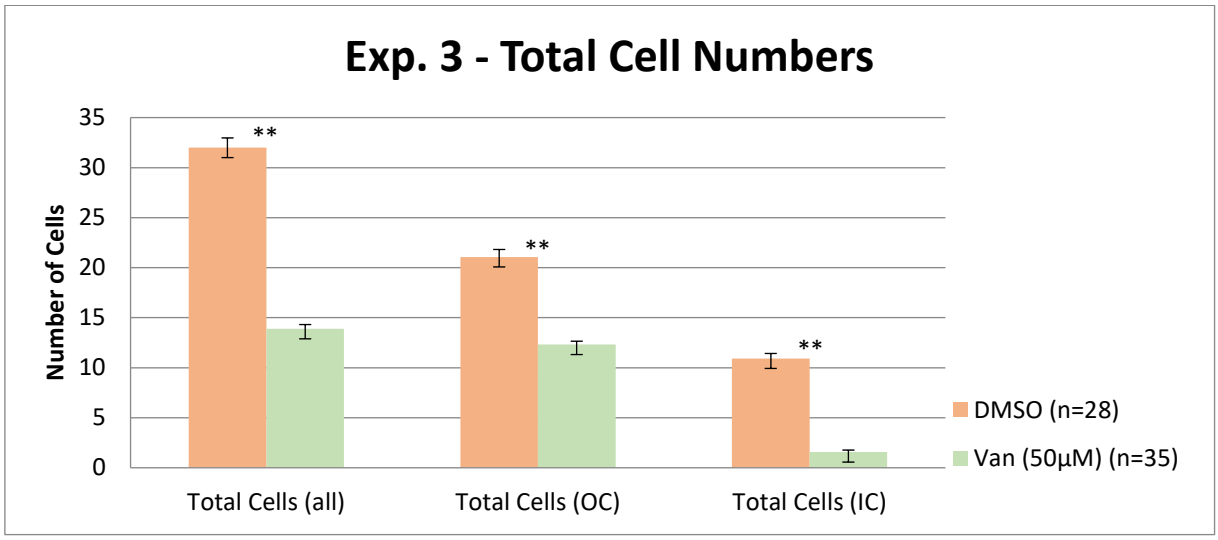

Figure.18 Average numbers of cells observed in the control group (DMSO) and the VEGFR2 inhibited group (Van), from experiment 1 (see also Table 3); plus either DMSO or Vandetanib (50µM) from E2.5 – E3.5. Comparison of the total numbers of cells as well as of inner (IC) and outer (OC) cells at the E3.5.

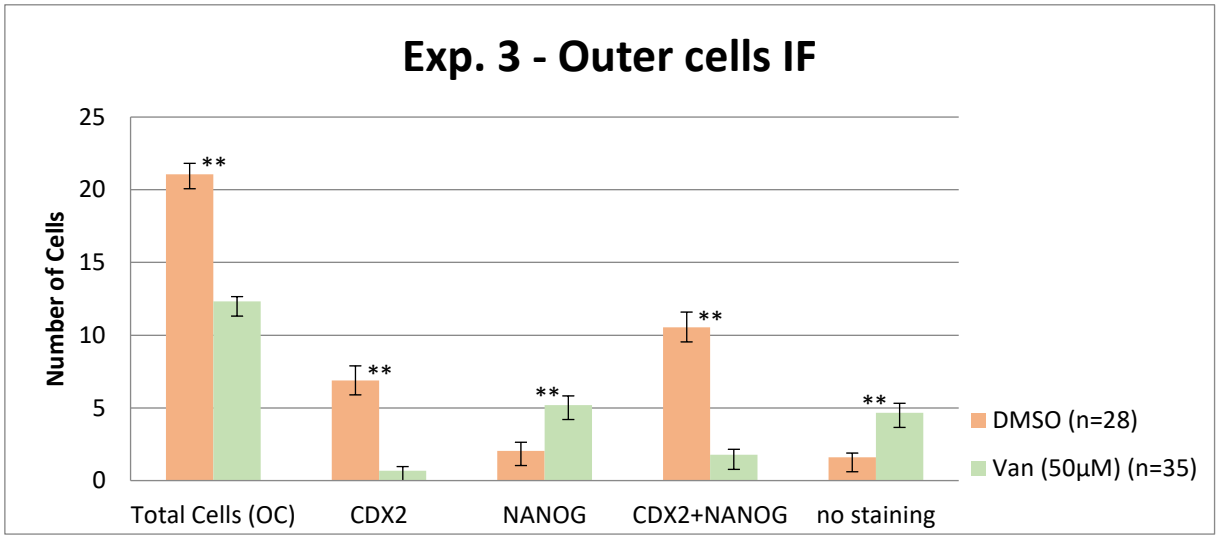

Figure 19. Average number of outer cells observed in the control group (DMSO) and inhibitor group (Van), from experiment 3; including a comparison of expression distribution of the TE marker, CDX2 and the EPI marker, Nanog. Potentially significant (*) and significant (**) differences between the groups are highlighted; two-tailed unpaired t-test, p-values < 0.05 and < 0.005, respectively.

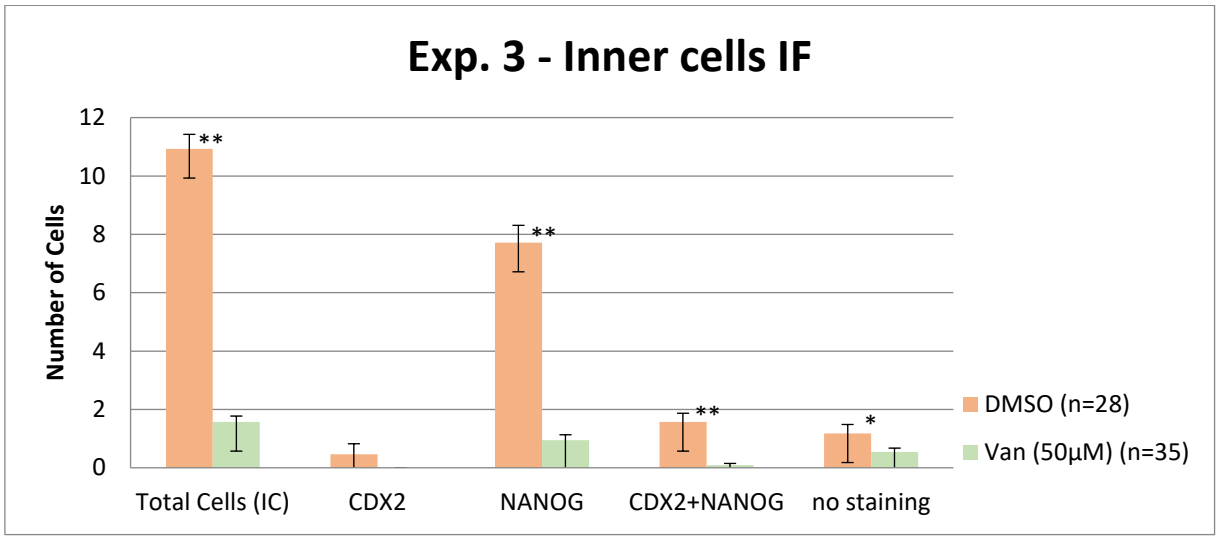

Figure 20. Average number of inner cells observed in the control group (DMSO) and inhibitor group (Van), from experiment 2; including a comparison of expression distribution of the TE marker, CDX2 and the EPI marker, NANOG. Potentially significant (*) and significant (**) differences between the groups are highlighted; two-tailed unpaired t-test, p-values < 0.05 and < 0.005, respectively.

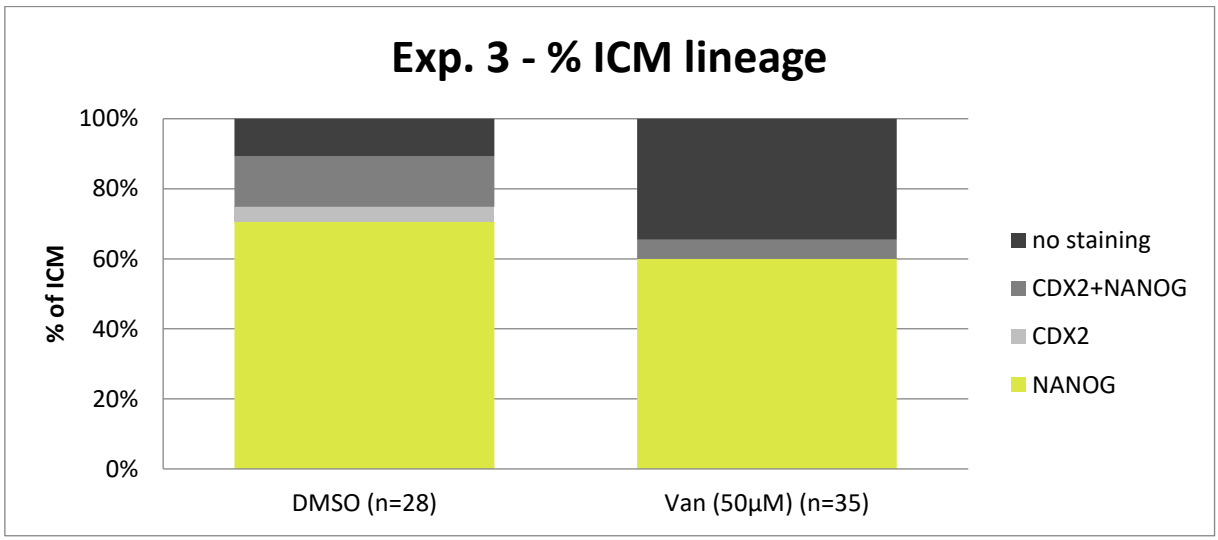

Figure 21. Average percentages of ICM assayed cells positively staining for examined lineage markers (or not) in relation to experiment 3.

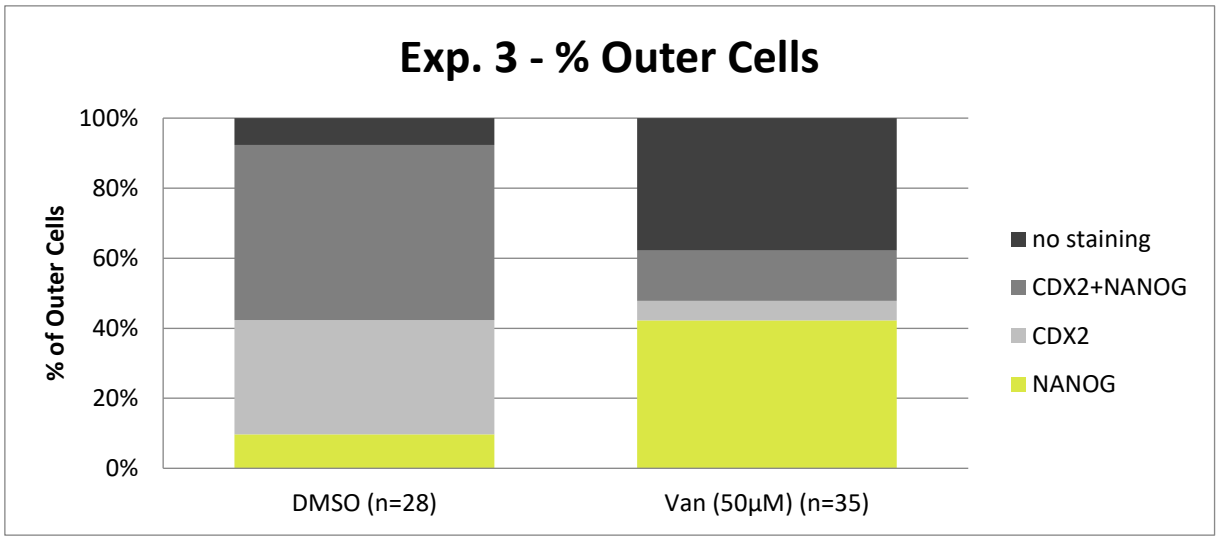

Figure 22. Average percentages of assayed outer cells positively staining for examined lineage markers (or not) in relation to experiment 3.

4.2. Effect of the highly concentrated VEGFR2 inhibitor

As described in experiment 3, Vandetanib has a strong inhibitory effect on the development of embryonic cells, and cell death induction was observed. There a two types of cell death, namely apoptosis and necrosis. Apoptosis is an orchestrated and regulated/ programmed elimination of cells by which energy is consumed to degrade the cell. In contrast, necrosis is a toxic mechanism, whereby the cell experiences a passive degradation without energy consumption and is directly damaged. Thus, we wanted to find out if Vandetanib triggered a controlled cell death, apoptosis, or if it was toxic to the cell and caused necrosis (Elmore, 2007).

4.2.1. Experiment 4 – Employing 50µM Vandetanib from E2.5 to E4.5 to study cell-death

To determine whether the blastomeres of the developmentally arrested Vandetanib-treated (using the high 50µM concentration) embryos undergo necrosis due to the potentially direct toxic effects of the high concentration of Vandetanib, or controlled cell death apoptosis induced by the cell itself as a response to the Vandetanib-induced changes (notably VEGFR2 inhibition), embryos were again *in vitro* cultured in 50µM Vandetanib, from E2.5 – E4.5 (the late blastocyst stage; this later stage was chosen to maximise the potential for observing dead/ dying cells consequent to the treatment) and immuno-fluorescently stained with an antibody against the apoptotic marker, cleaved CASPASE 3 (Figure 23).

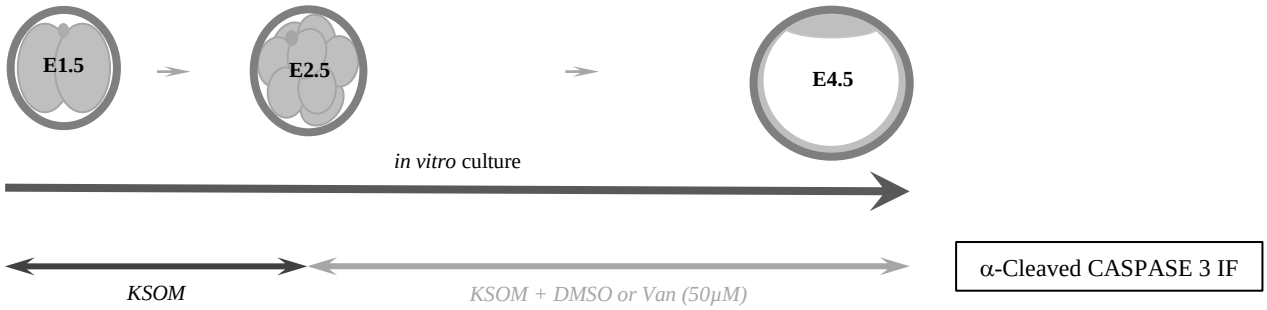

Figure 23. Schematic visualisation of the experiment 4. 2-cell stage (E1.5) embryos were cultured in KSOM media until the 8-cell stage (E2.5), then they were treated with DMSO or VEGFR2 inhibitor (50µM) and cultured in vitro until late blastocyst stage (E4.5) fixed and assayed for expression of the apoptotic cell death marker, cleaved CASPASE 3.

The result was consistent with that obtained in experiment 3, as the total number of cells in the VEGFR2 inhibitor treated group was dramatically and significantly decreased in comparison to the control group (Table 4 and Figure 24). Detailed analysis of the confocal micrographs, and the DAPI staining in particular (indicative of nuclei and hence cell number), revealed that the control embryos had developed in a developmentally appropriate fashion and were correctly staged and exhibited intact nuclei. In contrast, the DAPI-stained DNA of the treated groups was fragmented, thus indicating that the majority of nuclei were degraded (exemplar images given in Figure 25, A). In the inhibited cells, cleaved CASPASE 3 was also found in higher concentrations, as compared to the basal levels observed in the control group (Figure 25, B). The anti-cleaved CASPASE 3 immuno-reactivity did not present as a homogenously distributed pattern but was rather present in defined punctae; a further characteristic hall mark of apoptosis .Figure 25, C is a merged view of the overall immuno-fluorescently stained exemplar samples/ images. Overall, these results suggest that using Vandetanib in a concentration of 50µM, potentially acting solely via VEGFR2 inhibition, triggers apoptosis and therefore is not directly toxic to the cell.

	Total Cells (all)	Total Cells (OC)	Total Cells (IC)
DMSO	77.3 (9.1)	58.8 (7.7)	18.5 (2.7)
Vandetanib (50µM)	12 (0.7)	11.4 (0.7)	0.6 (0.2)
p-value[1]	2.44E-07**	1.12E-06**	5.73E-07**

Table 4. Values of Experiment 4. Average (±SEM) values for the average number of total cells and outer and inner cells of the DMSO control group (n=4) and 50µM Vandetanib group (n=9), when embryos were in vitro cultured from E2.5 to E4.5 in KSOM media with DMSO (control group) or Vandetanib (experimental group). Potentially significant (*) and significant (**) differences between the groups are highlighted; two-tailed unpaired t-test, p-values < 0.05 and < 0.005, respectively.

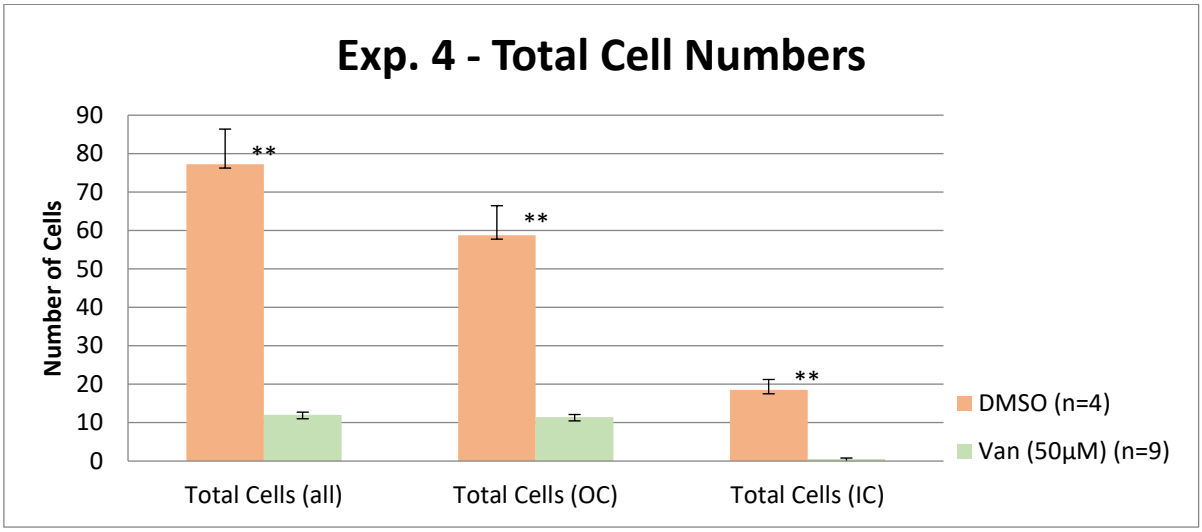

Figure 24. Average cell numbers of the control group (DMSO) and the inhibited group (Van) relating to experiment 4. Comparison of the total numbers of cells as well as of inner (IC) and outer (OC) cells at stage E4.5, is also provided. [1]Potentially significant (*) and significant (**) differences between the groups are highlighted; two-tailed unpaired t-test, p-values < 0.05 and < 0.005, respectively.

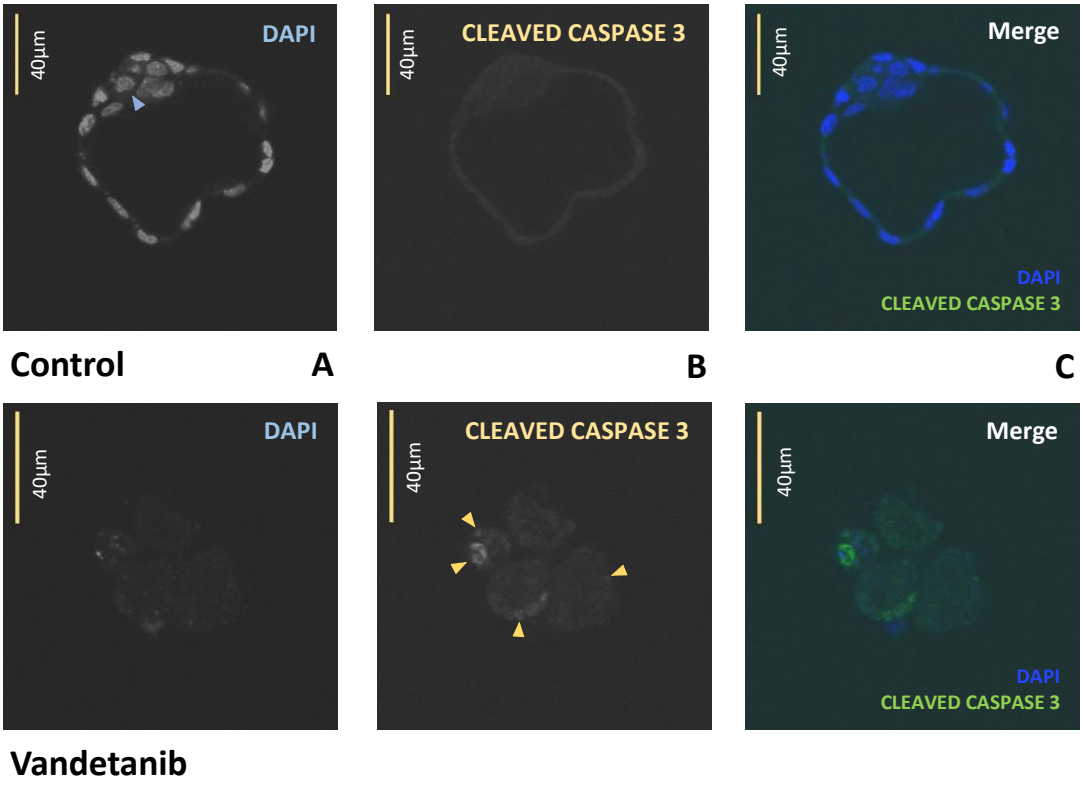

Figure 25. Confocal microscopy of stained embryos from Experiment 4. A. The exemplar micrographs show the staining of the DNA by DAPI. The blue arrow shows a proper nucleus in a cell of the well-developed ICM in the control group. In the treated group (Vandetanib), DNA is found in fragments. The staining of cleaved caspase 3 shows a weak/ basal background signal in the control group but is higher in the Vandetanib treated group; the distinct punctae/ distinct regions (indicated with yellow arrows). C. A merged view of both stains is depicted with DAPI in blue and cleaved caspase 3 in green.

4.3. Effects of VEGFR2 inhibition on the second cell fate decision

We next wanted to discover if the inhibition of VEGFR2 would have an effect on the second cell fate decision. The data from Graham *et al.* (2014b) showed that the amount of *Vegfr2* mRNA in inner cells is more than 2 times higher than in outer cells. Therefore, we hypothesized that the inhibition would have an effect mainly in the inner cells of developing mouse preimplantation embryos, from which the PrE and EPI lineages are derived. Therefore, we performed immuno-fluorescence staining of GATA4, a developmentally late lineage marker of committed PrE, and NANOG, specific for the EPI at E4.5, following VEGFR2 inhibition.

4.3.1. Experiment 5 – Using Vandetanib from E1.5 to E4.5 to assay ICM cell fates

Embryos were *in vitro* cultured in KSOM media containing a series of individual concentrations of Vandetanib, corresponding to values of 40nM, 400nM, 4µM, and 25µM (or a corresponding volume of DMSO in the culture group medium), from E1.5 to E4.5 (Figure 26).

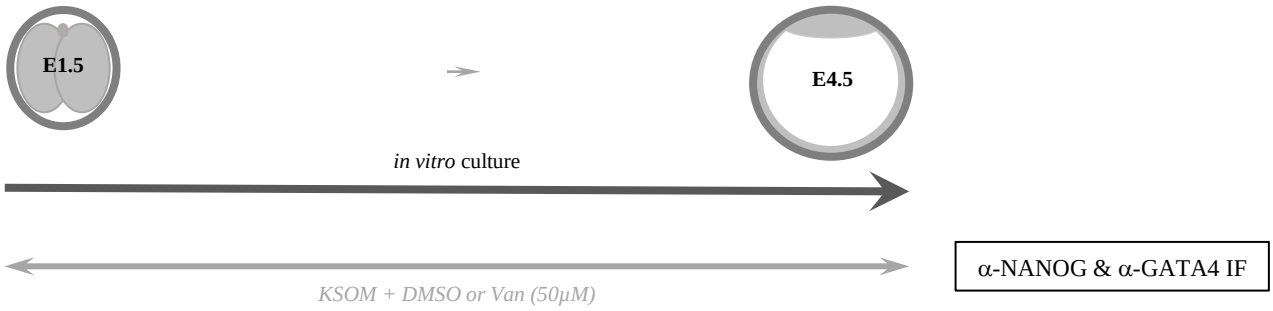

Figure 26. Schematic visualisation of experiment 5. Embryos were treated with DMSO or Vandetanib inhibitor (at various concentrations) and in vitro cultured from the 2-cell (E1.5) to late blastocyst stage (E4.5), fixed, and assayed for the presence of ICM linage markers, GATA4 (PrE) and NANOG (EPI) by immuno-fluorescent staining.

In the experiment, antibodies against GATA4 and NANOG had been used for immuno-fluorescence staining analysis, however in this instance the immuno-fluorescence staining against NANOG inexplicably failed (hence precluding a direct assay of EPI cells within the ICM). The reason for this is not clarified but could be related to the need to change to a second aliquot of previously untested secondary antibody. Nevertheless, from previous experiments it could be concluded that there was no profound effect that would be specific to the expression of the pluripotency marker NANOG *per se*, in the analyses of the first cell lineages segregation (Table 3): it is therefore likely that any effect examined in the context of the second cell fate

lineage specification/ segregation is also not profound. However, it is important to note that a repetition of the experiment could provide more direct information. Therefore, evaluation of the results was only possible in relation to the emergence of the GATA4 positive PrE lineage (Table 5 &. Figure 29) As can be seen, at lower concentrations, from 40nM to 4µM, the values showed no significant differences, neither in the total cell numbers nor in the average frequency of immuno-fluorescently labelled cells. However, in the group with the concentration of 25µM, the embryos were affected in a manner that was similar to that observed in experiment 2 (utilising 20µM Vandetanib). This was exemplified by a significant reduction in the total number of cells that affected both outer and inner cell populations (Figure 27 &Figure 28). The number of cells expressing GATA4 was also significantly decreased. However, despite all embryos being equally influenced by Vandetanib in terms of reduced cell number, a bias towards a specific lineage (*i.e.* presumed EPI or PrE) consequent to VEGFR2 inhibition could not be found, suggesting the increased amount of VEGFR2 mRNA observed by Graham *et al.* (2014b) in 16-cell stage inner cells may not have a function cell-fate consequence during preimplantation mouse embryo development.

		Outer Cells		Inner Cells	
	Total Cells (all)	**Total Cells**	**Gata4**	**Total Cells**	**Gata4**
DMSO	98.6 (4.4)	73.9 (3.4)	0 (0)	24.7 (1.2)	7.7 (0.9)
Vandetanib (40nM)	94.6 (3.1)	71.3 (2.6)	0 (0)	23.3 (1.1)	8.4 (0.7)
p-value[1]	5.96E-01	6.66E-01	5.50E-01	5.00E-01	6.27E-01
Vandetanib (400nM)	98.5 (2.1)	73.3 (2.3)	0 (0)	25.2 (1.5)	9.2 (1.2)
p-value[1]	9.92E-01	9.45E-01	6.45E-01	8.78E-01	4.54E-01
Vandetanib (4µM)	103.3 (3.1)	79.6 (2.2)	0 (0)	23.6 (1.3)	9.2 (0.7)
p-value[1]	4.41E-01	2.19E-01	4.34E-01	5.51E-01	2.28E-01
Vandetanib (25µM)	71.8 (4.6)	57.4 (3.5)	0 (0)	14.4 (1.6)	3.8 (0.9)
p-value[1]	1.65E-04**	2.16E-03**	4.08E-01	3.30E-06**	4.50E-03**

Table 5. Values of Experiment 5. Average (±SEM) values of total cells and outer and inner cells of DMSO control group (n=27), 40nM Van group (n=10), 400nM Van group (n=6), 4µM Van group (n=17), and 25µM Van group (n=19). The embryos were cultured from E1.5 to E4.5 in KSOM media with DMSO (control group) or Vandetanib (experimental group); at the indicated concentrations. Outer and inner cells judged by their relative spatial position within the embryo are categorised as staining positive for GATA4 alone. [1]Potentially significant (*) and significant (**) differences between the groups are highlighted; two-tailed unpaired t-test, p-values < 0.05 and < 0.005, respectively.

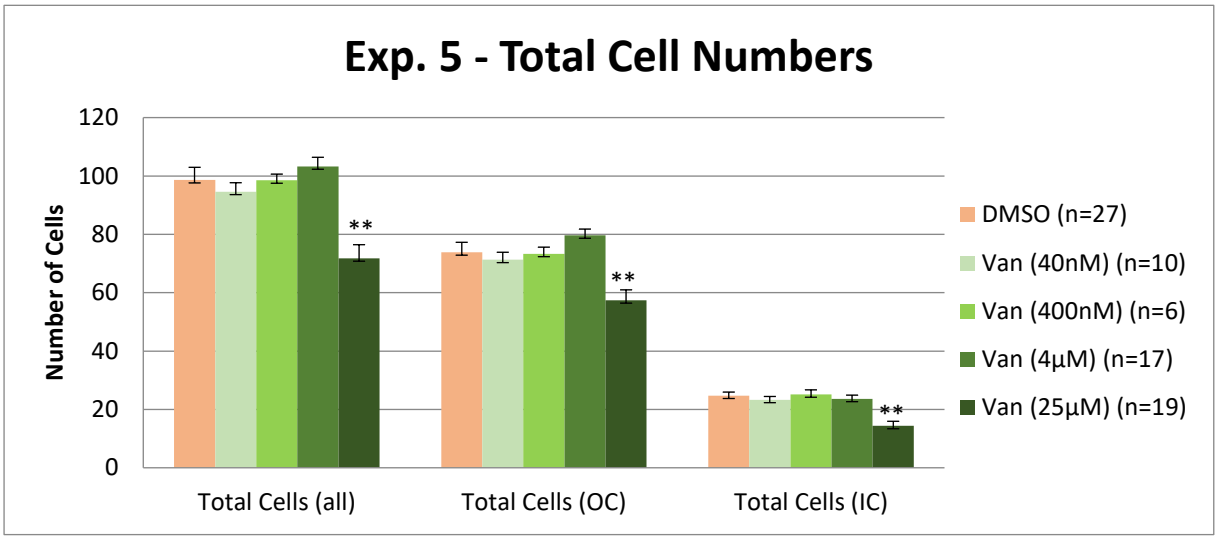

Figure 27. Average numbers of cells observed in the control group (DMSO) and the VEGFR2 inhibited groups (Van), at the indicated concentrations, from E1.5 – E4.5, in relation to experiment 5 (see also Table 5); Comparison of the total numbers of cells as well as of inner (IC) and outer (OC) cells at the E3.5 is given.

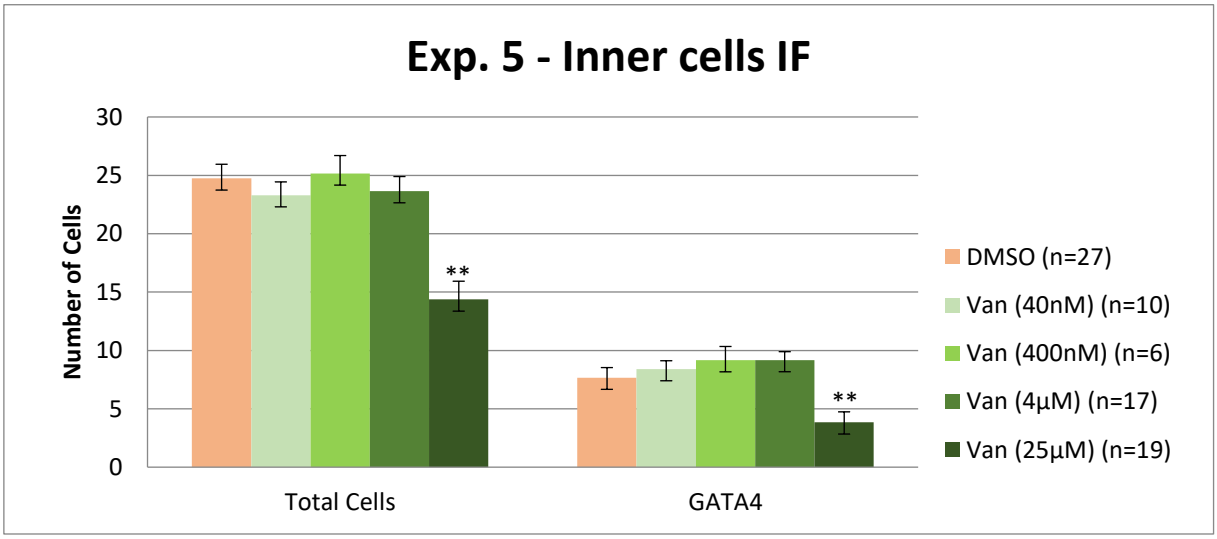

Figure 28. Average number of inner cells observed in the control group (DMSO) and inhibitor groups (Van), at the indicated concentration, from experiment 5; including a comparison of expression distribution of the PrE marker, GATA4. Potentially significant (*) and significant (**) differences between the groups are highlighted; two-tailed unpaired t-test, p-values < 0.05 and < 0.005, respectively.

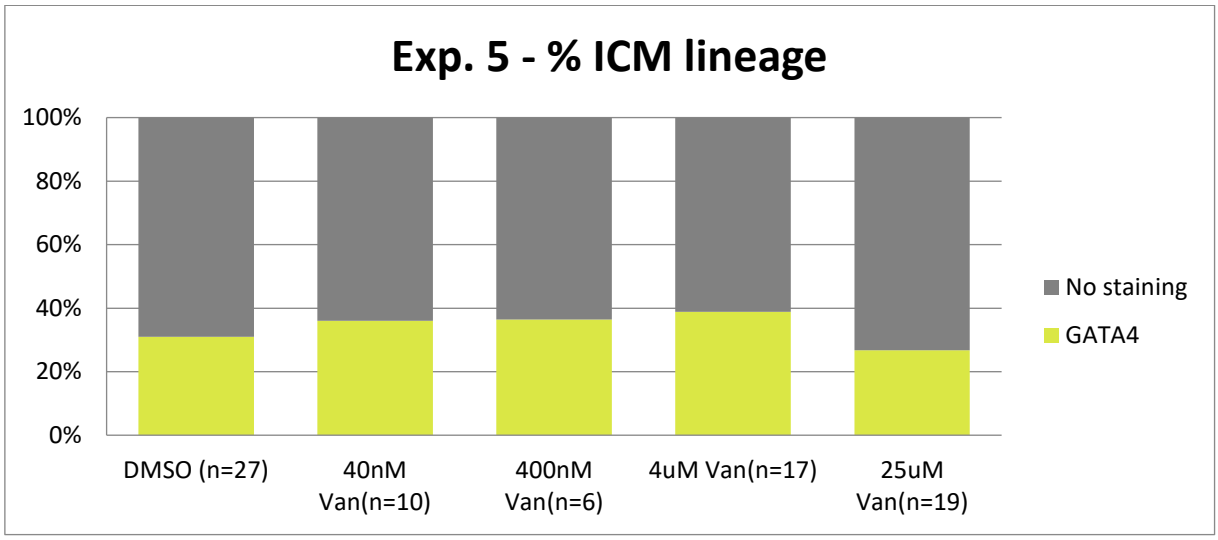

Figure 29. Average percentages of ICM assayed cells positively staining for examined lineage markers (or not) in relation to experiment 5.

4.4. Overall data summary and discussion

In the presented experiments, the effects of the inhibition of the VEGFR2 receptor in mouse preimplantation embryos have been studied, via culturing the embryos with the specific inhibitor Vandetanib. We have shown that a treatment with the inhibitor in concentrations below 20μM does not have an effect on the cell/ embryo development. However, embryo culture from E1.5 to E3.5 using a 20μM concentration of Vandetanib did report higher numbers of CDX2- and NANOG-positive double stained cells, concomitant with reduced numbers of specified outer TE cells expressing CDX2 alone. These data could be interpreted as evidence for reduced or delayed lineage segregation, given co-expression of these two lineage marker genes is indicative of unspecified cell fate. Indeed, a similar trend was also observed in inner cells, whereby the number of solely NANOG staining ICM cells was reduced whilst those positive for both NANOG and CDX2 were increased further strengthening the interpretation of impaired/ delayed cell-fate specification under these conditions. In another experiment, exploiting the Vandetanib inhibitor from E2.5 to E3.5, total cell numbers in both the TE and ICM lineages were shown to be reduced, however, the proportion of outer cells expressing Nanog alone was increased (while the ratio of cells only expressing the TE marker Cdx2 was lower). This suggests that the known regulatory relationship that governs the *Nanog* gene's transcription suppression by CDX2 in early mouse embryo outer TE cells (as stated by Strumpf (2005)) is active and furthermore,VEGFR2 can an influence the expression *Cdx2* in outer cells, as it's inhibition causes spatially ectopic *Nanog* expression. Furthermore, applying the inhibitor (20μM) from the 8-cell (E2.5) stage delayed general embryo development,

whereas higher doses of Vandetanib led to the induction of programmed apoptotic cell death (confirmed by cleaved CASPASE 3 immunofluorescence staining – Figure 22). This suggests that Vandetanib is not inherently toxic for cells, but stunts signalling, most probably via VEGFR2, that leads to the induction of apoptosis. Graham *et al*. (2014b) previously reported a higher expression of the VEGFR2 receptor in inner cells of the 16-cell (E3.0) stage embryo, suggesting a potential role of VEGFR2 within the ICM and potentially in the separation/ specification of the EPI and PrE lineages. However, we could not find any evidence from our data to support this hypothesis; albeit the experiment in question (number 5) was technically hindered by not being able to assay *Nanog* protein expression directly, as a readout of EPI cell specification. Hence, a further repletion of this experiment would be beneficial and recommended. Indeed, further studies exploiting prolonged incubation times using Vandetanib at the 20μM inhibitor concentration would also be useful to study further the uncovered first (and potentially second) cell fate decision delays observed (see experiment 1). On further consideration would be to obtain a second independent and distinct VEGFR2 inhibitor (or employ a different experimental strategy to cause its function disruption – *e.g.* microinjection of RNAi constructs targeting the VEGFR2 mRNA transcript for destruction) to test the potentially delayed specification phenotypes, as it has been reported that Vandetanib can also target, but at much lower potency, VEGFR3 and EGFR (epidermal growth factor receptor).

5. CONCLUSION

In this study a potential role for active VEGFR2 in cell fate specification during the preimplantation stages of mouse embryo development has been assayed using a chemical inhibition-based approach. The results provide evidence that VEGFR2 may exhibit regulative properties on the timing of cell lineage specification and that in the outer embryo compartment, some cells can inappropriately specify to an ICM cell lineage. At the present moment, there is no evidence that VEGFR2 inhibition adversely affects the derivation of the PrE lineage, although repetition of the relevant experiments (using a combination of anti-sera that recognise both PrE and EPI lineage markers within the same immuno-fluorescently stained blastocysts would be advisable – given the technical problem experienced and explained in this study).

6. REFERENCES

Alberts, Johnson, Lewis, Raff, Roberts, Walter Lefers, M. F.-F. T. (2009). *"Molecular Biology of the cell."*

Bischoff, M., Parfitt, D.-E., & Zernicka-Goetz, M. (2008). Formation of the embryonic-abembryonic axis of the mouse blastocyst: relationships between orientation of early cleavage divisions and pattern of symmetric/asymmetric divisions. *Development*, *135*(5), 953–962. https://doi.org/10.1242/dev.014316

Blij, S., Frum, T., Akyol, A., Fearon, E., & Ralston, A. (2012). Maternal Cdx2 is dispensable for mouse development. *Development*, *139*(21), 3969–3972. https://doi.org/10.1242/dev.086025

Bruce, A. W., & Zernicka-Goetz, M. (2010). Developmental control of the early mammalian embryo: Competition among heterogeneous cells that biases cell fate. *Current Opinion in Genetics and Development*, *20*(5), 485–491. https://doi.org/10.1016/j.gde.2010.05.006

Chazaud, C., & Yamanaka, Y. (2016). Lineage specification in the mouse preimplantation embryo. *Development*, *143*(7), 1063–1074. https://doi.org/10.1242/dev.128314

Chazaud, C., Yamanaka, Y., Pawson, T., & Rossant, J. (2006). Early Lineage Segregation between Epiblast and Primitive Endoderm in Mouse Blastocysts through the Grb2-MAPK Pathway. *Developmental Cell*, *10*(5), 615–624. https://doi.org/10.1016/j.devcel.2006.02.020

Dard, N., Louvet-Vallée, S., Santa-Maria, A., & Maro, B. (2004). Phosphorylation of ezrin on threonine T567 plays a crucial role during compaction in the mouse early embryo. *Developmental Biology*, *271*(1), 87–97. https://doi.org/10.1016/j.ydbio.2004.03.024

de Vries, W. N. (2004). Maternal -catenin and E-cadherin in mouse development. *Development*, *131*(18), 4435–4445. https://doi.org/10.1242/dev.01316

Ducibella, T., & Anderson, E. (1975). Cell shape and membrane changes in the eight-cell mouse embryo: Prerequisites for morphogenesis of the blastocyst. *Developmental Biology*, *47*(1), 45–58. https://doi.org/10.1016/0012-1606(75)90262-6

Dziadek, M. (1979). Cell differentiation in isolated inner cell masses of mouse blastocysts in vitro: onset of specific gene expression. *Journal of Embryology and Experimental Morphology*, *53*(1977), 367–379.

Elmore, S. (2007). Apoptosis: A Review of Programmed Cell Death. *Toxicologic Pathology*, *35*(4), 495–516. https://doi.org/10.1080/01926230701320337

Fierro-González, J. C., White, M. D., Silva, J. C., & Plachta, N. (2013). Cadherin-dependent filopodia control preimplantation embryo compaction. *Nature Cell Biology*, *15*(12), 1424–1433. https://doi.org/10.1038/ncb2875

Gilbert, S. F. (2014). *Developmental Biology*. Sunderland, MA: Sinauer.

Goldstein, B., & Macara, I. G. (2007). The PAR Proteins: Fundamental Players in Animal Cell Polarization. *Developmental Cell*, *13*(5), 609–622. https://doi.org/10.1016/j.devcel.2007.10.007

Graham, S. J. L., Wicher, K. B., Jedrusik, A., Guo, G., Herath, W., Robson, P., & Zernicka-Goetz, M. (2014a). BMP signalling regulates the pre-implantation development of extra-embryonic cell lineages in the mouse embryo. *Nature Communications*, *5*(May), 1–11. https://doi.org/10.1038/ncomms6667

Graham, S. J. L., Wicher, K. B., Jedrusik, A., Guo, G., Herath, W., Robson, P., & Zernicka-Goetz, M. (2014b). BMP signalling regulates the pre-implantation development of extra-embryonic cell lineages in the mouse embryo - Supplementary Dataset 2. *Nature Communications*, *5*(May). https://doi.org/10.1038/ncomms6667

Hart, A. H., Hartley, L., Ibrahim, M., & Robb, L. (2004). Identification, Cloning and Expression Analysis of the Pluripotency Promoting Nanog Genes in Mouse and Human. *Developmental Dynamics*, *230*(1), 187–198. https://doi.org/10.1002/dvdy.20034

Hillman, N., Sherman, M. I., & Graham, C. (1972). The effect of spatial arrangement on cell determination during mouse development. *Embryol. Exp. Morph*, *28*(2), 263–278.

Hyafil, F., Morello, D., Babinet, C., & Jacob, F. (1980). A cell surface glycoprotein involved in the compaction of embryonal carcinoma cells and cleavage stage embryos. *Cell*, *21*(3), 927–934. https://doi.org/10.1016/0092-8674(80)90456-0

Jedrusik, A., Cox, A., Wicher, K., Glover, D. M., & Zernicka-Goetz, M. (2015). Maternal-zygotic knockout reveals a critical role of Cdx2 in the morula to blastocyst transition. *Developmental Biology*, *398*(2), 147–152. https://doi.org/10.1016/j.ydbio.2014.12.004

Jedrusik, A., Parfitt, D. E., Guo, G., Skamagki, M., Grabarek, J. B., Johnson, M. H., … Zernicka-Goetz, M. (2008). Role of Cdx2 and cell polarity in cell allocation and specification of trophectoderm and inner cell mass in the mouse embryo. *Genes and Development*, *22*(19), 2692–2706. https://doi.org/10.1101/gad.486108

Johnson, M. H. (2009). From Mouse Egg to Mouse Embryo: Polarities, Axes, and Tissues. *Annual Review of Cell and Developmental Biology*, *25*(1), 483–512. https://doi.org/10.1146/annurev.cellbio.042308.113348

Johnson, M. H., & Ziomek, C. A. (1981). The foundation of two distinct cell lineages within the mouse morula. *Cell*, *24*(1), 71–80. https://doi.org/10.1016/0092-8674(81)90502-X

Kang, M., Piliszek, A., Artus, J., & Hadjantonakis, A.-K. (2013). FGF4 is required for lineage restriction and salt-and-pepper distribution of primitive endoderm factors but not their initial expression in the mouse. *Development*, *140*(2), 267–279. https://doi.org/10.1242/dev.084996

Kemphues, K. J., Priess, J. R., Morton, D. G., & Cheng, N. S. (1988). Identification of genes required for cytoplasmic localization in early C. elegans embryos. *Cell*, *52*(3), 311–320. https://doi.org/10.1016/S0092-8674(88)80024-2

Krawchuk, D., Honma-Yamanaka, N., Anani, S., & Yamanaka, Y. (2013). FGF4 is a limiting factor controlling the proportions of primitive endoderm and epiblast in the ICM of the mouse blastocyst. *Developmental Biology*, *384*(1), 65–71. https://doi.org/10.1016/j.ydbio.2013.09.023

Larue, L., Ohsugi, M., Hirchenhain, J., & Kemler, R. (1994). E-cadherin null mutant embryos fail to form a trophectoderm epithelium. *Proceedings of the National Academy of Sciences*, *91*(17), 8263–8267. https://doi.org/10.1073/pnas.91.17.8263

Leung, C. Y., & Zernicka-Goetz, M. (2015). Mapping the journey from totipotency to lineage specification in the mouse embryo. *Current Opinion in Genetics and Development*, *34*, 71–76. https://doi.org/10.1016/j.gde.2015.08.002

Louvet, S., Aghion, J., Santa-Maria, A., Mangeat, P., & Maro, B. (1996). Ezrin becomes restricted to outer cells following asymmetrical division in the preimplantation mouse embryo. *Developmental Biology*, *177*(2), 568–579. https://doi.org/10.1006/dbio.1996.0186

Mihajlović, A. I., & Bruce, A. W. (2017). The first cell-fate decision of mouse preimplantation embryo development: Integrating cell position and polarity. *Open Biology*, *7*(11). https://doi.org/10.1098/rsob.170210

Mihajlovic, A. I., Thamodaran, V., & Bruce, A. W. (2015). The first two cell-fate decisions of preimplantation mouse embryo development are not functionally independent. *Scientific Reports*, *5*(October), 1–16. https://doi.org/10.1038/srep15034

Morris, S. A., Graham, S. J. L., Jedrusik, A., & Zernicka-Goetz, M. (2013). The differential response to Fgf signalling in cells internalized at different times influences lineage segregation in preimplantation mouse embryos. *Open Biology*, *3*(NOV). https://doi.org/10.1098/rsob.130104

Morris, S. A., Guo, Y., & Zernicka-Goetz, M. (2012). Developmental Plasticity Is Bound by

Pluripotency and the Fgf and Wnt Signaling Pathways. *Cell Reports*, *2*(4), 756–765. https://doi.org/10.1016/j.celrep.2012.08.029

Morris, S. A., Teo, R. T. Y., Li, H., Robson, P., Glover, D. M., & Zernicka-Goetz, M. (2010). Origin and formation of the first two distinct cell types of the inner cell mass in the mouse embryo. *Proceedings of the National Academy of Sciences*, *107*(14), 6364–6369. https://doi.org/10.1073/pnas.0915063107

Morrisey, E. E., Tang, Z., Sigrist, K., Lu, M. M., Jiang, F., Ip, H. S., & Parmacek, M. S. (1998). GATA6 regulates HNF4 and is required for differentiation of visceral endoderm in the mouse embryo. *Genes and Development*, *12*(22), 3579–3590. https://doi.org/10.1101/gad.12.22.3579

Nagy, A., Gertsenstein, M., Vintersten, K., & Behringer, R. (2003). *Manipulating the Mouse Embryo*. *Cold Spring Harbor, NY: Cold Spring Harbor Laboratory Press* (THIRD EDIT). Cold Spring Harbor Laboratory Press.

Olsson, A. K., Dimberg, A., Kreuger, J., & Claesson-Welsh, L. (2006). VEGF receptor signalling - In control of vascular function. *Nature Reviews Molecular Cell Biology*, *7*(5), 359–371. https://doi.org/10.1038/nrm1911

Perrino, C., & Rockman, H. A. (2006). GATA4 and the two sides of gene expression reprogramming. *Circulation Research*, *98*(6), 715–716. https://doi.org/10.1161/01.RES.0000217593.07196.af

Plusa, B. (2005). Downregulation of Par3 and aPKC function directs cells towards the ICM in the preimplantation mouse embryo. *Journal of Cell Science*, *118*(3), 505–515. https://doi.org/10.1242/jcs.01666

Saiz, N., & Plusa, B. (2013). Early cell fate decisions in the mouse embryo. *Reproduction*, *145*(3), R65–R80. https://doi.org/10.1530/REP-12-0381

Schultz, R. M. (1993). Regulation of zygotic gene activation in the mouse. *BioEssays*, *15*(8), 531–538. https://doi.org/10.1002/bies.950150806

Strumpf, D. (2005). Cdx2 is required for correct cell fate specification and differentiation of trophectoderm in the mouse blastocyst. *Development*, *132*(9), 2093–2102. https://doi.org/10.1242/dev.01801

Sutherland, A. E., Speed, T. P., & Calarco, P. G. (1990). Inner cell allocation in the mouse morula: The role of oriented division during fourth cleavage. *Developmental Biology*, *137*(1), 13–25. https://doi.org/10.1016/0012-1606(90)90003-2

Suwińska, A., Czołowska, R., Ozdzeński, W., & Tarkowski, A. K. (2008). Blastomeres of the mouse embryo lose totipotency after the fifth cleavage division: Expression of Cdx2

and Oct4 and developmental potential of inner and outer blastomeres of 16- and 32-cell embryos. *Developmental Biology*, *322*(1), 133–144. https://doi.org/10.1016/j.ydbio.2008.07.019

Tarkowski, A. K., & Wróblewska, J. (1967). Development of blastomeres of mouse eggs isolated at the 4- and 8-cell stage. *Journal of Embryology and Experimental Morphology*, *18*(1), 155–180.

Wang, W., Huang, J., & Chen, J. (2011). Angiomotin-like proteins associate with and negatively regulate YAP1. *Journal of Biological Chemistry*, *286*(6), 4364–4370. https://doi.org/10.1074/jbc.C110.205401

White, M. D., & Plachta, N. (2015). *How adhesion forms the early mammalian embryo. Current Topics in Developmental Biology* (1st ed., Vol. 112). Elsevier Inc. https://doi.org/10.1016/bs.ctdb.2014.11.022

Wicklow, E., Blij, S., Frum, T., Hirate, Y., Lang, R. A., Sasaki, H., & Ralston, A. (2014). HIPPO Pathway Members Restrict SOX2 to the Inner Cell Mass Where It Promotes ICM Fates in the Mouse Blastocyst. *PLoS Genetics*, *10*(10). https://doi.org/10.1371/journal.pgen.1004618

Yagi, R., Kohn, M. J., Karavanova, I., Kaneko, K. J., Vullhorst, D., DePamphilis, M. L., & Buonanno, A. (2007). Transcription factor TEAD4 specifies the trophectoderm lineage at the beginning of mammalian development. *Development*, *134*(21), 3827–3836. https://doi.org/10.1242/dev.010223

Yamanaka, Y., Lanner, F., & Rossant, J. (2010). FGF signal-dependent segregation of primitive endoderm and epiblast in the mouse blastocyst. *Development*, *137*(5), 715–724. https://doi.org/10.1242/dev.043471

Yamanaka, Y., Ralston, A., Stephenson, R. O., & Rossant, J. (2006). Cell and molecular regulation of the mouse blastocyst. *Developmental Dynamics*, *235*(9), 2301–2314. https://doi.org/10.1002/dvdy.20844

Zernicka-Goetz, M., Morris, S. A., & Bruce, A. W. (2009). Making a firm decision: Multifaceted regulation of cell fate in the early mouse embryo. *Nature Reviews Genetics*, *10*(7), 467–477. https://doi.org/10.1038/nrg2564

Zhao, B., Li, L., Lu, Q., Wang, L. H., Liu, C. Y., Lei, Q., & Guan, K. L. (2011). Angiomotin is a novel Hippo pathway component that inhibits YAP oncoprotein. *Genes and Development*, *25*(1), 51–63. https://doi.org/10.1101/gad.2000111

Ziomek, C. A., & Johnson, M. H. (1980). Cell surface interaction induces polarization of mouse 8-cell blastomeres at compaction. *Cell*, *21*(3), 935–942.

https://doi.org/10.1016/0092-8674(80)90457-2

Ziomek, C. A., Johnson, M. H., & Handyside, A. H. (1982). The developmental potential of mouse 16-cell blastomeres. *Journal of Experimental Zoology*, *221*(3), 345–355. https://doi.org/10.1002/jez.1402210310

7. APPENDIX

Table 6. Counts of cell numbers and statistical values from experiment 1, control group (E1.5-E3.5).

		Outer Cells					Inner Cells				
Embryo Nb.	Total Cells	Total Cells	Cdx2	Nanog	Cdx2 + Nanog	Not Stained	Total Cells	Cdx2	Nanog	Cdx2 + Nanog	Not Stained
1	31	19	9	0	10	0	12	1	6	2	3
2	35	23	14	2	3	4	12	2	7	1	2
3	29	20	7	1	9	3	9	0	7	1	1
4	27	17	7	0	10	0	10	0	9	1	0
5	38	24	16	0	4	4	14	1	8	0	5
6	26	17	0	2	9	6	9	0	4	1	4
7	32	24	9	2	12	1	8	1	5	2	0
8	30	21	4	5	9	3	9	1	6	0	2
9	32	17	11	0	6	0	15	1	10	3	1
10	30	19	11	2	4	2	11	3	5	3	0
11	41	29	20	7	2	0	12	0	12	0	0
12	31	20	9	1	5	5	11	0	8	1	2
13	30	19	8	1	10	0	11	0	10	1	0
14	31	21	17	1	2	1	10	0	7	1	2
15	23	11	6	1	2	2	12	0	9	3	0
16	33	19	4	2	10	3	14	0	9	3	2
17	31	18	6	0	12	0	13	0	12	0	1
18	27	16	0	3	10	3	11	0	5	2	4
19	26	16	2	1	11	2	10	0	7	0	3
TOTAL	**583**	**370**	**160**	**31**	**140**	**39**	**213**	**10**	**146**	**25**	**32**
AVERAGE	**30.7**	**19.5**	**8.4**	**1.6**	**7.4**	**2.1**	**11.2**	**0.5**	**7.7**	**1.3**	**1.7**
SEM	**1.0**	**0.9**	**1.3**	**0.4**	**0.8**	**0.4**	**0.4**	**0.2**	**0.5**	**0.3**	**0.4**

Table 7. Counts of cell numbers and statistical values from experiment 1, inhibitor group (E1.5-E3.5), 20µM Vandetanib.

		Outer Cells					Inner Cells				
Embryo Nb.	Total Cells	Total Cells	Cdx2	Nanog	Cdx2 + Nanog	Not Stained	Total Cells	Cdx2	Nanog	Cdx2 + Nanog	Not Stained
1	24	16	1	0	12	3	8	0	0	6	2
2	31	21	3	0	17	1	10	0	7	2	1
3	34	21	0	0	18	3	13	1	9	3	0
4	32	24	14	2	8	0	8	2	6	0	0
5	32	18	8	1	9	0	14	1	13	0	0
6	32	21	6	15	0	0	11	9	1	1	0
7	24	13	0	0	13	0	11	1	1	9	0
8	33	22	4	1	16	1	11	0	5	6	0
9	29	17	0	0	17	0	12	1	8	3	0
TOTAL	**271**	**173**	**36**	**19**	**110**	**8**	**98**	**15**	**50**	**30**	**3**
AVERAGE	**30.1**	**19.2**	**4.0**	**2.1**	**12.2**	**0.9**	**10.9**	**1.7**	**5.6**	**3.3**	**0.3**
SEM	**1.2**	**1.2**	**1.6**	**1.6**	**1.9**	**0.4**	**0.7**	**0.9**	**1.4**	**1.0**	**0.2**
P-VALUE	**7.3E-01**	**8.7E-01**	**4.9E-02**	**7.1E-01**	**1.2E-02**	**1.0E-01**	**6.9E-01**	**1.1E-01**	**9.8E-02**	**1.6E-02**	**2.1E-02**

Table 8. Counts of cell numbers and statistical values from experiment 2, control group (E2.5-E3.5).

		Outer Cells					Inner Cells				
Embryo Nb.	Total Cells	Total Cells	Cdx2	Nanog	Cdx2 + Nanog	Not Stained	Total Cells	Cdx2	Nanog	Cdx2 + Nanog	Not Stained
1	34	21	6	1	14	0	13	0	11	0	2
2	21	16	3	1	10	2	5	0	3	1	1
3	29	19	5	1	13	0	10	0	6	4	0
4	30	21	15	0	6	0	9	0	8	0	1
5	35	23	6	0	15	2	12	1	9	0	2
6	30	20	7	12	1	0	10	1	5	4	0
7	31	21	3	0	17	1	10	0	7	3	0
8	27	17	3	1	13	0	10	0	8	2	0
9	29	19	3	0	16	0	10	0	7	3	0
10	31	20	3	0	17	0	11	0	7	4	0
11	24	17	4	0	13	0	7	0	5	0	2
12	31	24	9	0	14	1	7	1	5	1	0
13	31	21	4	0	13	4	10	1	4	0	5
14	26	16	2	1	10	3	10	0	9	0	1
15	37	25	0	0	19	6	12	0	6	3	3
16	31	20	0	3	15	2	11	0	7	0	4
17	22	15	0	3	3	9	7	0	5	0	2
TOTAL	**499**	**335**	**73**	**23**	**209**	**30**	**164**	**4**	**112**	**25**	**23**
AVERAGE	**29.4**	**19.7**	**4.3**	**1.4**	**12.3**	**1.8**	**9.6**	**0.2**	**6.6**	**1.5**	**1.4**
SEM	**1.0**	**0.7**	**0.9**	**0.7**	**1.2**	**0.6**	**0.5**	**0.1**	**0.5**	**0.4**	**0.4**

Table 9. Counts of cell numbers and statistical values from experiment 2, inhibitor group (E2.5-E3.5), 20µM Vandetanib.

		Outer Cells					Inner Cells				
Embryo Nb.	Total Cells	Total Cells	Cdx2	Nanog	Cdx2 + Nanog	Not Stained	Total Cells	Cdx2	Nanog	Cdx2 + Nanog	Not Stained
1	32	21	3	0	18	0	11	1	8	1	1
2	33	21	0	3	18	0	12	0	11	1	0
3	31	17	2	0	14	1	14	1	10	3	0
4	19	12	4	0	7	1	7	0	6	0	1
5	26	18	7	0	11	0	8	0	5	1	2
6	28	17	5	3	7	2	11	0	11	0	0
7	29	18	3	0	15	0	11	0	9	1	1
8	28	22	5	0	17	0	6	0	2	4	0
9	35	23	5	2	15	1	12	0	9	2	1
10	32	22	0	2	18	2	10	0	8	2	0
11	11	11	1	4	4	2	0	0	0	0	0
12	13	11	0	2	0	9	2	0	0	0	2
13	15	13	2	3	0	8	2	0	1	0	1
14	17	15	1	8	0	6	2	0	2	0	0
15	15	15	1	7	2	5	0	0	0	0	0
16	16	13	0	4	7	2	3	0	3	0	0
17	13	11	4	2	0	5	2	0	0	0	2
18	16	14	0	8	5	1	2	0	2	0	0
19	16	16	0	10	4	2	0	0	0	0	0
20	16	13	0	9	4	0	3	0	2	0	1
21	18	15	0	12	1	2	3	0	3	0	0
22	15	13	0	3	0	10	2	0	1	0	1
23	13	11	0	6	2	3	2	0	2	0	0
TOTAL	**487**	**362**	**43**	**88**	**169**	**62**	**125**	**2**	**95**	**15**	**13**
AVERAGE	**21.2**	**15.7**	**1.9**	**3.8**	**7.3**	**2.7**	**5.4**	**0.1**	**4.1**	**0.7**	**0.6**
SEM	**1.7**	**0.8**	**0.5**	**0.8**	**1.4**	**0.6**	**1.0**	**0.1**	**0.8**	**0.2**	**0.2**
P-VALUE	**4.6E-04**	**1.1E-03**	**1.3E-02**	**2.6E-02**	**1.5E-02**	**3.1E-01**	**1.2E-03**	**2.0E-01**	**2.4E-02**	**7.0E-02**	**3.7E-02**

Table 10. Counts of cell numbers and statistical values from experiment 3, control group (E2.5-E3.5).

		Outer Cells					Inner Cells				
Embryo Nb.	**Total Cells**	**Total Cells**	**Cdx2**	**Nanog**	**Cdx2 + Nanog**	**Not Stained**	**Total Cells**	**Cdx2**	**Nanog**	**Cdx2 + Nanog**	**Not Stained**
1	32	16	7	0	6	3	16	0	11	2	3
2	32	21	15	0	6	0	11	0	8	3	0
3	33	20	4	1	14	1	13	0	9	3	1
4	32	22	14	0	7	1	10	0	9	1	0
5	47	34	14	4	14	2	13	0	8	1	4
6	32	20	0	10	7	3	12	0	12	0	0
7	34	23	6	2	10	5	11	0	11	0	0
8	16	14	1	9	1	3	2	0	2	0	0
9	31	20	9	1	9	1	11	0	9	1	1
10	30	19	0	6	12	1	11	0	10	1	0
11	31	19	8	0	7	4	12	0	12	0	0
12	35	27	9	3	10	5	8	0	7	1	0
13	30	22	15	2	5	0	8	0	7	1	0
14	32	21	14	0	5	2	11	1	3	2	5
15	31	19	10	0	8	1	12	1	9	2	0
16	38	25	15	1	8	1	13	0	9	0	4
17	30	19	4	0	15	0	11	0	9	2	0
18	31	19	10	1	8	0	12	0	8	1	3
19	28	18	5	1	11	1	10	0	10	0	0
20	30	21	12	0	6	3	9	0	9	0	0
21	32	21	7	11	3	0	11	1	6	2	2
22	31	20	6	3	10	1	11	10	1	0	0
23	27	19	3	0	16	0	8	0	6	1	1
24	31	18	1	0	17	0	13	0	10	3	0
25	29	19	0	2	17	0	10	0	7	2	1
26	39	29	2	0	25	2	10	0	3	4	3
27	39	23	2	0	19	2	16	0	10	5	1
28	33	22	0	0	19	3	11	0	1	6	4
TOTAL	**896**	**590**	**193**	**57**	**295**	**45**	**306**	**13**	**216**	**44**	**33**
AVERAGE	**32.0**	**21.1**	**6.9**	**2.0**	**10.5**	**1.6**	**10.9**	**0.5**	**7.7**	**1.6**	**1.2**
SEM	**1.0**	**0.7**	**1.0**	**0.6**	**1.1**	**0.3**	**0.5**	**0.4**	**0.6**	**0.3**	**0.3**

Table 11. Counts of cell numbers and statistical values from experiment 3, inhibitor group (E2.5-E3.5), 50µM Vandetanib.

		Outer Cells					Inner Cells				
Embryo Nb.	Total Cells	Total Cells	Cdx2	Nanog	Cdx2 + Nanog	Not Stained	Total Cells	Cdx2	Nanog	Cdx2 + Nanog	Not Stained
1	11	11	1	4	4	2	0	0	0	0	0
2	13	11	0	2	0	9	2	0	0	0	2
3	15	13	2	3	0	8	2	0	1	0	1
4	17	15	1	8	0	6	2	0	2	0	0
5	15	15	1	7	2	5	0	0	0	0	0
6	16	13	0	4	7	2	3	0	3	0	0
7	13	11	4	2	0	5	2	0	0	0	2
8	16	14	0	8	5	1	2	0	2	0	0
9	16	16	0	10	4	2	0	0	0	0	0
10	16	13	0	9	4	0	3	0	2	0	1
11	18	15	0	12	1	2	3	0	3	0	0
12	15	13	0	3	0	10	2	0	1	0	1
13	13	11	0	6	2	3	2	0	2	0	0
14	14	13	2	1	0	10	1	0	0	0	1
15	14	12	1	5	0	6	2	0	0	0	2
16	15	13	0	7	1	5	2	0	0	0	2
17	16	13	0	10	2	1	3	0	1	0	2
18	8	8	0	3	4	1	0	0	0	0	0
19	12	10	0	1	8	1	2	0	2	0	0
20	15	12	0	9	1	2	3	0	3	0	0
21	13	13	0	10	2	1	0	0	0	0	0
22	16	13	0	10	2	1	3	0	3	0	0
23	14	14	0	8	6	0	0	0	0	0	0
24	16	14	0	3	0	11	2	0	1	0	1
25	11	9	0	5	2	2	2	0	2	0	0
26	17	13	8	0	1	4	4	0	2	2	0
27	11	10	4	0	0	6	1	0	0	0	1
28	13	13	0	0	0	13	0	0	0	0	0
29	9	9	0	2	0	7	0	0	0	0	0
30	15	14	0	12	0	2	1	0	1	0	0
31	15	12	0	6	4	2	3	0	2	1	0
32	12	11	0	6	0	5	1	0	0	0	1
33	17	15	0	0	0	15	2	0	0	0	2
34	9	9	0	5	0	4	0	0	0	0	0
35	10	10	0	1	0	9	0	0	0	0	0
TOTAL	**486**	**431**	**24**	**182**	**62**	**163**	**55**	**0**	**33**	**3**	**19**
AVERAGE	**13.9**	**12.3**	**0.7**	**5.2**	**1.8**	**4.7**	**1.6**	**0.0**	**0.9**	**0.1**	**0.5**
SEM	**0.4**	**0.3**	**0.3**	**0.6**	**0.4**	**0.7**	**0.2**	**0.0**	**0.2**	**0.1**	**0.1**
P-VALUE	**1.5E-26**	**7.9E-17**	**1.1E-08**	**6.4E-04**	**6.8E-12**	**2.4E-04**	**4.3E-27**	**1.5E-01**	**1.6E-17**	**1.1E-06**	**4.4E-02**

Table 12. Counts of cell numbers and statistical values from experiment 4, control group (E2.5-E4.5).

Embryo Nb.	Total Cells	Total Cells (OC)	Total Cells (IC)
1	58	44	14
2	88	73	15
3	97	71	26
4	66	47	19
TOTAL	**309**	**235**	**74**
AVERAGE	**77.3**	**58.8**	**18.5**
SEM	**9.1**	**7.7**	**2.7**

Table 13. Counts of cell numbers and statistical values from experiment 4, inhibitor group (E2.5-E4.5), 50µM Vandetanib.

Embryo Nb.	Total Cells	Total Cells (OC)	Total Cells (IC)
1	16	15	1
2	10	9	1
3	9	9	0
4	11	10	1
5	14	12	2
6	13	13	0
7	13	13	0
8	11	11	0
9	11	11	0
TOTAL	**108**	**103**	**5**
AVERAGE	**12.0**	**11.4**	**0.6**
SEM	**0.7**	**0.7**	**0.2**
P-VALUE	**2.4E-07**	**1.1E-06**	**5.7E-07**

Table 14. Counts of cell numbers and statistical values from experiment 5, control group (E1.5-E4.5).

		Outer Cells		Inner Cells	
Embryo Nb.	Total Cells	Total Cells	Gata4	Total Cells	Gata4
1	76	58	0	18	9
2	80	60	0	20	10
3	93	65	1	28	9
4	94	72	0	22	9
5	94	67	0	27	5
6	96	69	0	27	9
7	164	122	0	42	17
8	136	104	0	32	13
9	119	92	0	27	16
10	121	90	0	31	9
11	124	88	0	36	10
12	122	95	0	27	11
13	107	80	0	27	7
14	72	53	0	19	1
15	107	79	0	28	9
16	70	57	0	13	0
17	81	67	0	14	0
18	66	45	0	21	5
19	103	82	0	21	7
20	90	66	0	24	3
21	90	64	0	26	13
22	110	82	0	28	11
23	90	65	0	25	6
24	78	54	0	24	1
25	115	94	0	21	7
26	80	61	0	19	7
27	84	63	0	21	3
TOTAL	**2662**	**1994**	**1**	**668**	**207**
AVERAGE	**98.6**	**73.9**	**0.0**	**24.7**	**7.7**
SEM	**4.4**	**3.4**	**0.0**	**1.2**	**0.9**

Table 15. Counts of cell numbers and statistical values from experiment 5, inhibitor group (E1.5-E4.5), 40nM Vandetanib.

		Outer Cells		Inner Cells	
Embryo Nb.	Total Cells	Total Cells	Gata4	Total Cells	Gata4
1	82	61	0	21	10
2	83	63	0	20	5
3	88	65	0	23	10
4	94	78	0	16	6
5	94	69	0	25	10
6	107	82	0	25	11
7	107	78	0	29	10
8	101	77	0	24	8
9	104	78	0	26	5
10	86	62	0	24	9
TOTAL	**946**	**713**	**0**	**233**	**84**
AVERAGE	**94.6**	**71.3**	**0.0**	**23.3**	**8.4**
SEM	**3.1**	**2.6**	**0.0**	**1.1**	**0.7**
P-VALUE	**6.0E-01**	**6.7E-01**	**5.5E-01**	**5.0E-01**	**6.3E-01**

Table 16. Counts of cell numbers and statistical values from experiment 5, inhibitor group (E1.5-E4.5), 400nM Vandetanib.

		Outer Cells		Inner Cells	
Embryo Nb.	Total Cells	Total Cells	Gata4	Total Cells	Gata4
1	94	78	0	16	6
2	107	81	0	26	10
3	102	74	0	28	14
4	102	73	0	29	13
5	98	74	0	24	6
6	88	60	0	28	6
TOTAL	**591**	**440**	**0**	**151**	**55**
AVERAGE	**98.5**	**73.3**	**0.0**	**25.2**	**9.2**
SEM	**2.1**	**2.3**	**0.0**	**1.5**	**1.2**
P-VALUE	**9.9E-01**	**9.4E-01**	**6.4E-01**	**8.8E-01**	**4.5E-01**

Table 17. Counts of cell numbers and statistical values from experiment 5, inhibitor group (E1.5-E4.5), 4µM Vandetanib.

		Outer Cells		Inner Cells	
Embryo Nb.	Total Cells	Total Cells	Gata4	Total Cells	Gata4
1	99	78	0	21	8
2	93	72	0	21	7
3	97	77	0	20	12
4	92	72	0	20	8
5	91	74	0	17	8
6	97	75	0	22	6
7	93	69	0	24	7
8	115	93	0	22	12
9	106	82	0	24	7
10	82	67	0	15	4
11	105	77	0	28	9
12	108	84	0	24	9
13	112	85	0	27	9
14	107	84	0	23	13
15	136	99	0	37	16
16	119	92	0	27	12
17	104	74	0	30	9
TOTAL	**1756**	**1354**	**0**	**402**	**156**
AVERAGE	**103.3**	**79.6**	**0.0**	**23.6**	**9.2**
SEM	**3.1**	**2.2**	**0.0**	**1.3**	**0.7**
P-VALUE	**4.4E-01**	**2.2E-01**	**4.3E-01**	**5.5E-01**	**2.3E-01**

Table 18. Counts of cell numbers and statistical values from experiment 5, inhibitor group (E1.5-E4.5), 25µM Vandetanib.

		Outer Cells		Inner Cells	
Embryo Nb.	Total Cells	Total Cells	Gata4	Total Cells	Gata4
1	51	43	0	8	0
2	54	47	0	7	0
3	70	58	0	12	2
4	35	27	0	8	0
5	59	51	0	8	0
6	84	78	0	6	5
7	39	32	0	7	0
8	94	70	0	24	9
9	78	58	0	20	2
10	98	74	0	24	8
11	54	45	0	9	0
12	60	51	0	9	0
13	107	85	0	22	11
14	87	61	0	26	9
15	74	61	0	13	5
16	80	62	0	18	7
17	63	48	0	15	2
18	84	63	0	21	9
19	93	77	0	16	4
TOTAL	**1364**	**1091**	**0**	**273**	**73**
AVERAGE	**71.8**	**57.4**	**0.0**	**14.4**	**3.8**
SEM	**4.6**	**3.5**	**0.0**	**1.6**	**0.9**
P-VALUE	**1.6E-04**	**2.2E-03**	**4.1E-01**	**3.3E-06**	**4.5E-03**